Australian Government

Department of Sustainability, Environment, Water, Population and Communities
Supervising Scientist

internal report **618**

Assessment of expected maximum doses from the El Sherana airstrip containment, South Alligator River valley, Australia

Andreas Bollhöfer, Che Doering,

Peter Medley, Linda da Costa

July 2013

Release status – unrestricted

Project number –MON-2013-006

This page has been left blank intentionally.

Assessment of expected maximum doses from the El Sherana airstrip containment, South Alligator River valley, Australia

Andreas Bollhöfer, Che Doering, Peter Medley, Linda da Costa

Supervising Scientist Division

GPO Box 461, Darwin NT 0801

July 2013

Project number MON-2013-006

Registry File SG2005/0127

(Release status – unrestricted)

Australian Government

Department of Sustainability, Environment, Water, Population and Communities

Supervising Scientist

How to cite this report:

Bollhöfer A, Doering C, Medley P & da Costa L 2013. Assessment of expected maximum doses from the El Sherana airstrip containment, South Alligator River valley, Australia. Internal Report 618, July, Supervising Scientist, Darwin.

Project number – MON-2013-006

Location of final PDF file in SSDX Sharepoint/SPIRE:

Supervising Scientist Division>PublicationWork>Publications and Productions>InternalReports (IRs)>Nos 600 to 699>IR618 Dose Constrain El Sherana (Bollhöfer et al)

Authors of this report:

Andreas Bollhöfer – Environmental Research Institute of the Supervising Scientist, GPO Box 461, Darwin NT 0801, Australia

Che Doering – Environmental Research Institute of the Supervising Scientist, GPO Box 461, Darwin NT 0801, Australia

Peter Medley – Environmental Research Institute of the Supervising Scientist, GPO Box 461, Darwin NT 0801, Australia

Linda da Costa – Environmental Research Institute of the Supervising Scientist, GPO Box 461, Darwin NT 0801, Australia

The Supervising Scientist is part of the Australian Government Department of Sustainability, Environment, Water, Population and Communities.

Supervising Scientist
Department of Sustainability, Environment, Water, Population and Communities
GPO Box 461, Darwin NT 0801 Australia

e-mail: enquiries_ssd@environment.gov.au

Internet: www.environment.gov.au/ssd (www.environment.gov.au/ssd/publications)

Printed and bound in Darwin NT by Supervising Scientist Division

Contents

List of Figures

List of Tables

Executive summary

The El Sherana airstrip containment is a near-surface disposal facility located in the South Alligator Valley area in the south of Kakadu National Park. The containment was constructed, filled and covered in the 2009 dry season. It is currently in the institutional control period. This is the period following closure of the facility during which public access to, or alternative use of, the site must be restricted (NHMRC 1993). The containment is managed by Parks Australia with regulatory oversight by the Australian Radiation Protection and Nuclear Safety Agency (ARPANSA). An inspection of Parks Australia by ARPANSA on 27–28 September 2011 highlighted that dose constraints for the containment had not been established. Parks Australia subsequently requested that SSD conduct an assessment of potential doses to workers and the public from the containment that could be used to guide decision making on dose constraints.

Two scenarios were considered. The occupational scenario assumed that a Park Ranger spends 80 hours per year working onsite at the containment for routine maintenance. The member of the public scenario assumed that a tourist camped for four nights (40 hours in total) next to the boundary fence of the containment.

The dose from external gamma radiation was calculated by multiplying the 99th percentile of the above background dose rate with the time spent on site. The dose from radon progeny inhalation was calculated using the RESRAD-Offsite computer model, with the 99th percentile of the above background radon exhalation flux density used to determine the radon progeny concentration in air on and downwind of the containment for highly stable atmospheric conditions. The ingestion and dust inhalation pathways have not been considered. The expected maximum doses to a worker and a member of the public from the containment for the assumed exposure scenarios is less than 10 µSv per year for the current radiological characteristics of the containment.

1 Background

The El Sherana airstrip containment is a near-surface disposal facility located in the South Alligator River valley in the south of Kakadu National Park. It was constructed in the 2009 dry season and contains approximately 22,000 m^3 of naturally occurring radioactive material (NORM) contaminated waste from the remediation of legacy uranium mining and processing sites in the area (see Waggitt 2004) for details of the uranium mining history of the South Alligator River valley). Table 1 gives the engineering details of the containment.

The 2009 remediation of legacy uranium mining and processing sites and construction of the containment occurred as part of the 1996 lease agreement between the Gunlom Aboriginal Land Trust and the Director of National Parks and Wildlife (now the Director of National Parks) for traditional Aboriginal lands in the upper South Alligator River valley to be managed as part of Kakadu National Park. In particular, the lease agreement required the lessee to develop and fully implement a remediation plan which, in essence, would return the area to near to natural environmental status by the end of 2015. Parks Australia was the Australian Government agency responsible for development and implementation of the plan and was allocated $7.3 million over four years in the 2006–07 Federal Budget specifically for the programme (Director of National Parks 2006). The 2009 remediation works and construction of the containment represent major milestones in the lease agreement.

The ***eriss*** Environmental Radioactivity program has measured gamma dose rates and ^{222}Rn activity flux densities at the containment site prior to construction and again in 2010 one year after closure (Doering et al 2011). Gamma dose rates and ^{222}Rn activity flux densities were also measured in September 2012 as part of an ongoing (biannual) monitoring program. The purpose of this program is to assess whether the radiological conditions at the containment are stable, and to assess the performance of the containment through time. The 2012 measurements are presented in this report and are used to make an assessment of expected maximum annual doses for occupational and public exposure scenarios.

Table 1 Engineering details of the El Sherana airstrip containment.[1]

Parameter	Description
Surface footprint	8750 m^2 (175 m × 50 m)
Maximum capacity	25,000 m^3
Maximum excavation depth below natural ground level	5 m
Side slopes	3:1 (horizontal:vertical)
Maximum thickness of waste material	4.5 m
Base layer	0.5 m compacted clay
Capping layer	0.5 m compacted clay
Cover (growth medium)	1.8–2.4 m uncompacted natural soil

[1]Information from O'Kane Consultants (2012)

2 Methods

2.1 External gamma radiation measurements

A gamma survey was conducted at the containment on 3–4 September 2012 using three identical monitors with compensated Geiger Müller (GM) tubes. Measurements were made of the total counts per 100 s in air at a height of 1 m above the ground surface. A total of 274 measurements were made: 202 within the fenced area of the containment; 33 south of the fenced area; and 39 north of the fenced area.

One of the monitors was calibrated in December 2012. The calibration certificate for this monitor is shown in Figure A1 in Appendix 1. An intercomparison of the three monitors was conducted in the field to cross-calibrate them. Details of the monitors including the results of the cross-calibrations are shown in Table A1 in Appendix 1.

2.2 ^{222}Rn activity flux density measurements

^{222}Rn activity flux density measurements at the containment were made over the period 3–5 September 2012. The prevailing meteorological conditions over the measurement period were typical of the tropical Northern Territory dry season, with maximum daytime temperatures above 30°C and zero rainfall.

Brass canisters containing activated charcoal to entrap radon emanating from the ground surface were used for the field sampling of ^{222}Rn. Fourty three canisters were deployed on and around the containment. The canisters were embedded in the ground surface to a depth of approximately 1 cm in order to ensure a good seal and prevent leakage of radon from the canister to the atmosphere. Three additional canisters were carried into the field but remained sealed at all times. These canisters were 'controls' and used to determine the background activity of ^{222}Rn collected on the charcoal.

The ^{222}Rn activity flux density was calculated from the measured ^{222}Rn progeny activity in the canisters according to the method described in Doering et al (2011) and Spehr & Johnston (1983). The ^{222}Rn progeny activity in each canister was counted for ten minutes using a sodium iodide detector and the resulting energy spectrum displayed on a multi-channel analyser. Regions of interest were established around the characteristic photopeaks of ^{214}Pb - 214 (242 keV, 295 keV and 352 keV) and ^{214}Bi (609 keV) from which the net count rate was determined by adding the total counts under each peak for the individual field samples and then subtracting the mean sum of the counts under the corresponding regions of interest in the control canisters' spectra. The efficiency of the detector for ^{222}Rn progeny counting via this method is approximately 10.8%.

2.3 Measurement of the ^{226}Ra soil activity concentration

Soil samples from the top 5 cm were collected from directly underneath the planted radon cups at 17 locations on the containment (ie above the buried waste) after retrieval of the radon cups. This was principally done to determine the ^{226}Ra activity concentration in those soils and the relationship with ^{222}Rn activity flux density.

Soil radionuclide activity concentrations were measured using the high purity germanium gamma detectors of the ***eriss*** Environmental Radioactivity program. Approximately 15 g of sample were pressed into a standard geometry and then measured on the detectors to give ^{238}U, ^{226}Ra, ^{228}Ra, ^{228}Th, ^{210}Pb and ^{40}K activities in the samples. In-house procedures for sample collection, preparation and measurement via gamma spectrometry are described in Marten (1992) and Pfitzner (2010). An in-house program was used for analysis of sample radionuclide activity concentrations (Esparon & Pfitzner 2010).

The stability and background of the detectors are checked weekly with a multi-isotope standard containing radionuclides of the uranium and thorium decay chains and a blank matrix (empty container), respectively. Detection limits for soil samples using gamma spectrometry are dependent on sample size, detector efficiency and background count rates of the given nuclide, but are typically ~3 $Bqkg^{-1}$ for ^{226}Ra for a one day count in the present study.

3 Results and Discussion

3.1 External gamma radiation

External gamma dose rates were measured two years before construction of the containment in June 2007 (baseline), one year after construction in September 2010 and three years after construction in September 2012. The results of the 2012 measurements are given in Table A2 in Appendix 2. The results of the baseline and 2010 measurements are given in Doering et al (2011).

Figure 1 shows the location and magnitude of the baseline (left) and 2012 (right) gamma dose rate measurements at the containment site overlaid on an aerial photograph of the area from March 2007. The outer white rectangle indicates the approximate location of the boundary fence around the containment. The inner rectangle shows the approximate location of the containment and buried waste.

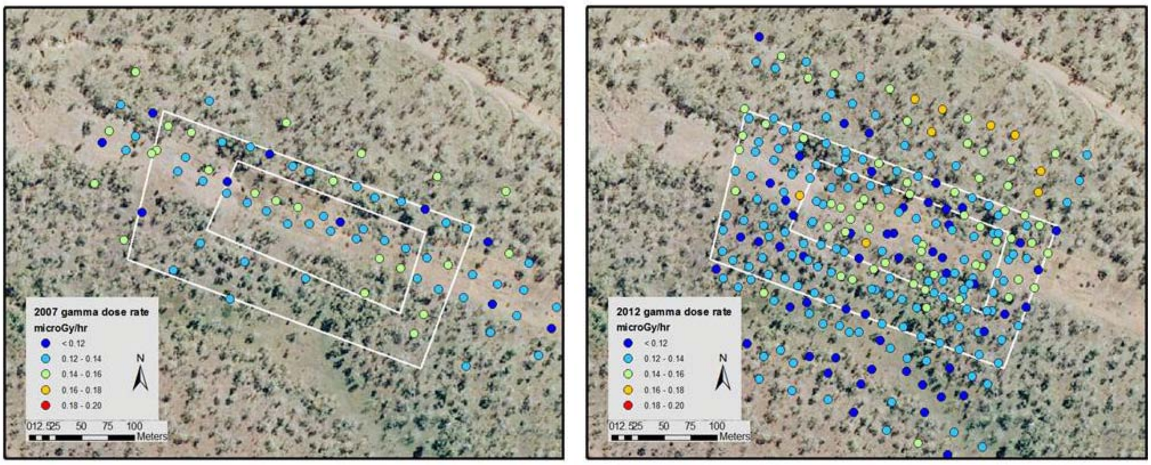

Figure 1: 2007 (baseline) and 2012 external gamma dose rates [$\mu Gy \cdot hr^{-1}$] measured at the El Sherana containment.

It has been shown that the baseline gamma dose rate measurements were normally distributed, with an average value inside the fenced area of 0.13±0.01 $\mu Gy \cdot hr^{-1}$ (Bollhöfer et al 2009). This is the same as the average value inside the fenced area from the 2012 measurements, meaning that the mean (50th percentile) above baseline gamma dose rate three years after construction is zero (Figure 2). The frequency distribution plot can also be used to determine the 99th percentile, which is 0.03 $\mu Gy \cdot hr^{-1}$. This means that less than 1% of the measured values is more than 0.03 $\mu Gy \cdot hr^{-1}$ above the baseline value.

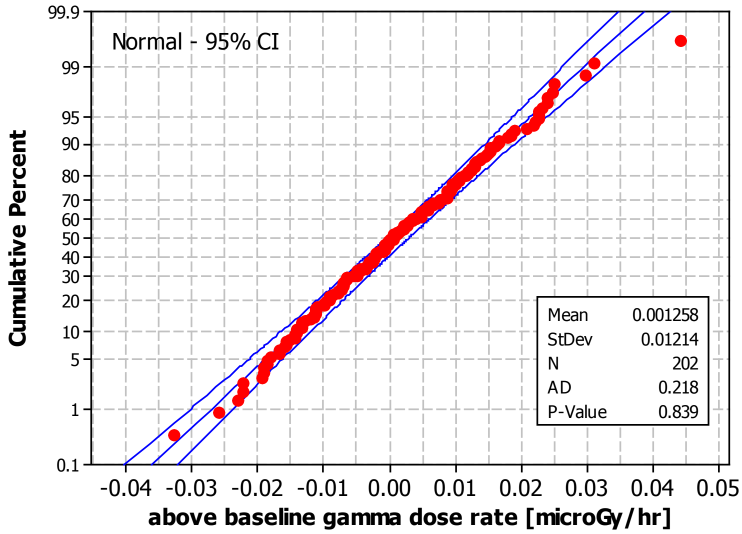

Figure 2 Frequency distribution of above baseline gamma dose rates [μGy·hr^{-1}] measured at the El Sherana containment in September 2012. N: number of measurements; AD: Anderson-Darling statistic.

3.2 ^{222}Rn activity flux densities

^{222}Rn activity flux densities were measured before construction of the containment in July 2009 (baseline), one year after construction in September 2010 and three years after construction in September 2012. The results of the 2012 measurements are given in Table A3 in Appendix 3. The results of the baseline and 2010 measurements are given in Doering et al (2011).

The average baseline ^{222}Rn activity flux density measured in July 2009 was 14 mBq·m^{2}·s^{-1}. Figure 3 shows the location and magnitude of post-construction ^{222}Rn activity flux density measurements conducted in 2010 (left) (Doering et al 2011) and in 2012 (right) at the containment overlaid on an aerial photograph of the area from March 2007. The outer white rectangle indicates the approximate location of the boundary fence around the containment. The inner rectangle shows the approximate location of the containment and buried waste.

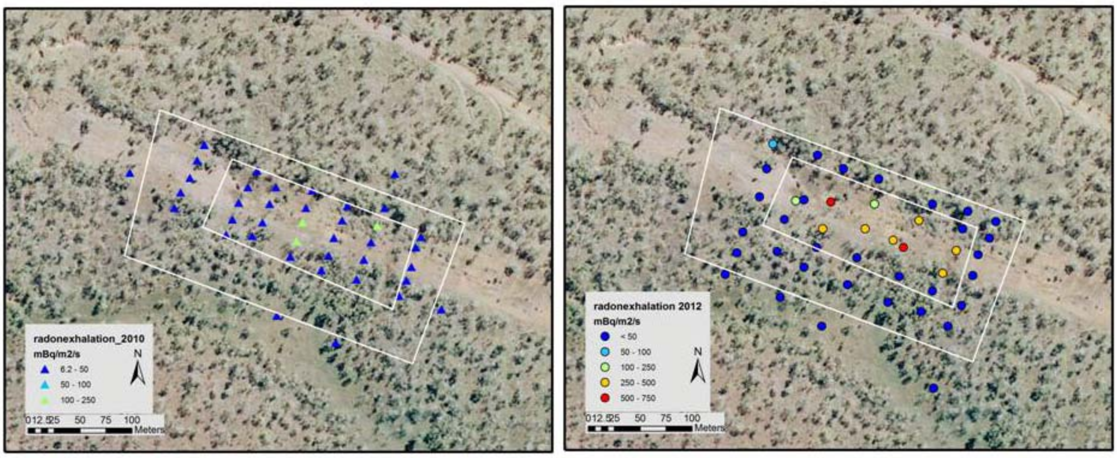

Figure 3: ^{222}Rn activity flux densities [mBq·m^{-2}·s^{-1}] measured at the El Sherana airstrip containment in September 2010 (left) and September 2012 (right).

^{222}Rn activity flux densities measured on the containment in 2012 were higher than those measured in 2010, but there has been little change in ^{222}Rn activity flux densities outside the fenced area at the control sites. The typical value measured in 2010 outside the fenced area was 16 mBqm ^{2}·s^{-1} (similar to the baseline value of 14 mBq·m^{2}·s^{-1}measured in 2009) with values ranging from 10–36 mBq·m^{2}·s^{-1}. In 2012, the typical value outside the fenced area was 21 mBq·m^{2}·s^{-1}, with a range of 9–30 mBq·m^{2}·s^{-1}. The average of the baseline and background measurements combined from the three years is 17 mBq·m^{2}·s^{-1}.

It has been shown that exhalation of radon in the natural environment follows a log-normal distribution (e.g. Bollhöfer et al 2005; Lawrence et al 2009), in accordance with the Theory of Successive Random Dilutions, which is in particular appropriate for inert substances (such as radon) released at relatively high concentrations into carrier media (Ott, 1995). Figure 4 shows histograms of the 2009 baseline ^{222}Rn activity flux density measurements and of the 2010 and 2012 ^{222}Rn activity flux density measurements from within the fenced area only. In 2009, the measurements followed a log-normal distribution. Although the histograms suggest that the measurements in 2010 and 2012 are also log-normally distributed, probability plots shown in Figure 5 show that this is not the case (p-value < 0.005). In particular, the 2012 measurements show a distinct bimodal distribution, with three quarters of values below 60 mBq·m^{2}·s^{-1} and one quarter above 200 mBq·m^{2}·s^{-1}. Hence, the 99th percentile has not been determined using the log-normal distribution fitted to the entire 2012 data in Figure 5.

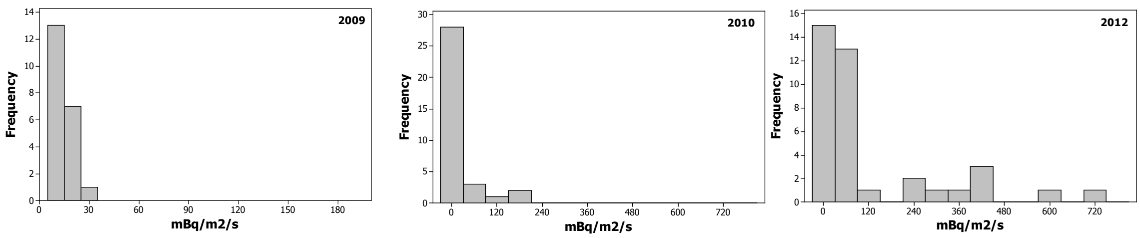

Figure 4: Histograms of the 2009 baseline, the 2010 and 2012 ^{222}Rn activity flux density measurements from within the fenced area.

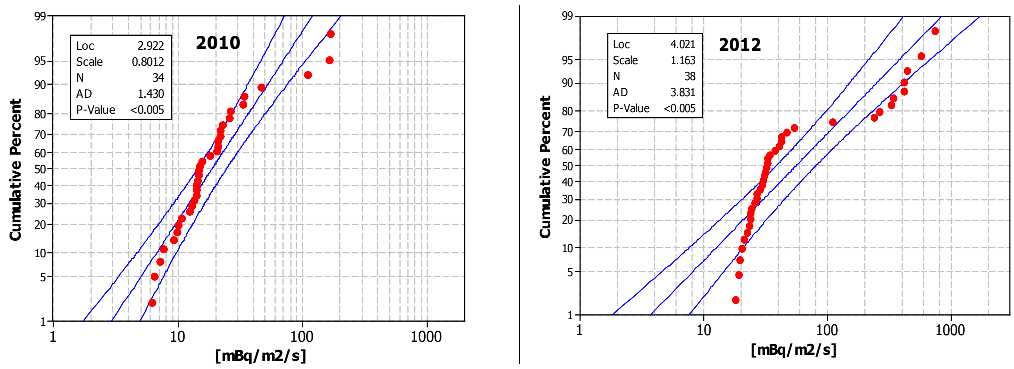

Figure 5: Frequency distribution of ^{222}Rn activity flux densities measured in September 2010 and 2012 at the El Sherana containment. P-values for the log-normal distribution are < 0.005, suggesting that the data are not from log-normally distributed populations. This is in particular obvious for the 2012 data.

Above baseline ^{222}Rn activity flux densities have been calculated by subtracting the average of the baseline and background ^{222}Rn activity flux density measurements (17 mBq·m^{-2}·s^{-1}) from the measurements conducted within the fenced area in 2012. Figure 6 shows the frequency distribution plot of the above baseline ^{222}Rn activity flux densities measured in 2012 with a log-normal distribution fitted to the total data population and individual log-normal distributions fitted to above baseline ^{222}Rn flux densities less than 40 mBq·m^{-2}·s^{-1} (population 1) and greater than 200 mBq·m^{-2}·s^{-1} (population 2), respectively. Sampling points of population 2 were all located centrally on top of the buried waste. Sampling points of population 1 were located at the edges or off the buried waste (Figure 3). Individual populations follow a log-normal distribution. Mean (50th percentile) above background ^{222}Rn activity flux densities are 10 mBqm $^{-2}$·s^{-1} and 380 mBqm $^{-2}$·s^{-1} for populations 1 and 2, respectively.

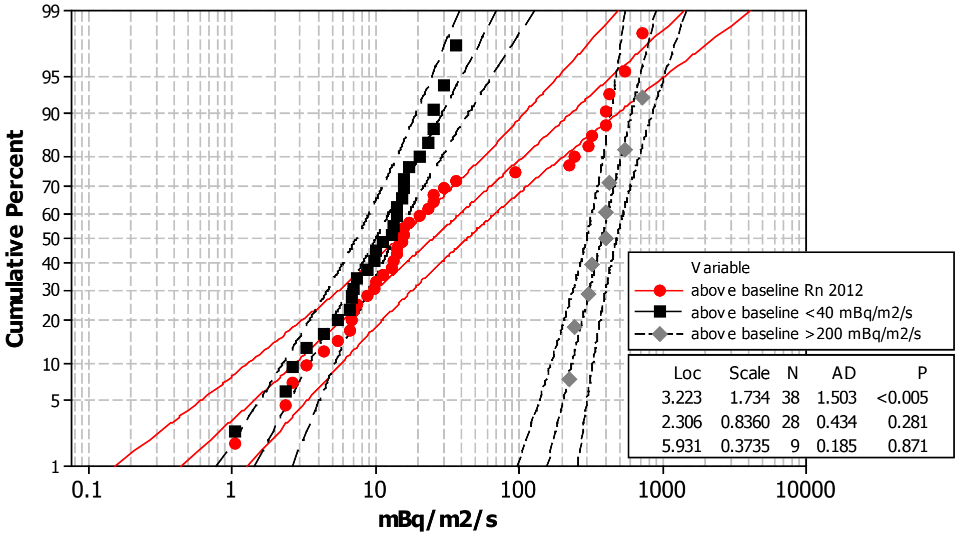

Figure 6: Probability plot of above baseline ^{222}Rn activity flux densities measured in 2012 for the total population (red), population 1 (<40 mBq·m^{-2}·s^{-1}, black squares) and population 2 (>200 mBq·m^{-2}·s^{-1}, grey diamonds). P-values for the log-normal distributions fitted to populations 1 and 2 are larger than 0.05 and AD statistics are low, suggesting that data are log-normally distributed around two modes. Loc and Scale are the location and scale parameters of the log-normal distribution.

3.3 ^{226}Ra soil activity concentrations

Figure 7 (left) shows the location of the soil samples taken and the magnitude of measured ^{226}Ra soil activity concentrations at the containment overlaid on an aerial photograph of the area from March 2007. The outer white rectangle indicates the approximate location of the boundary fence around the containment. The inner rectangle shows the approximate location of the containment and buried waste.

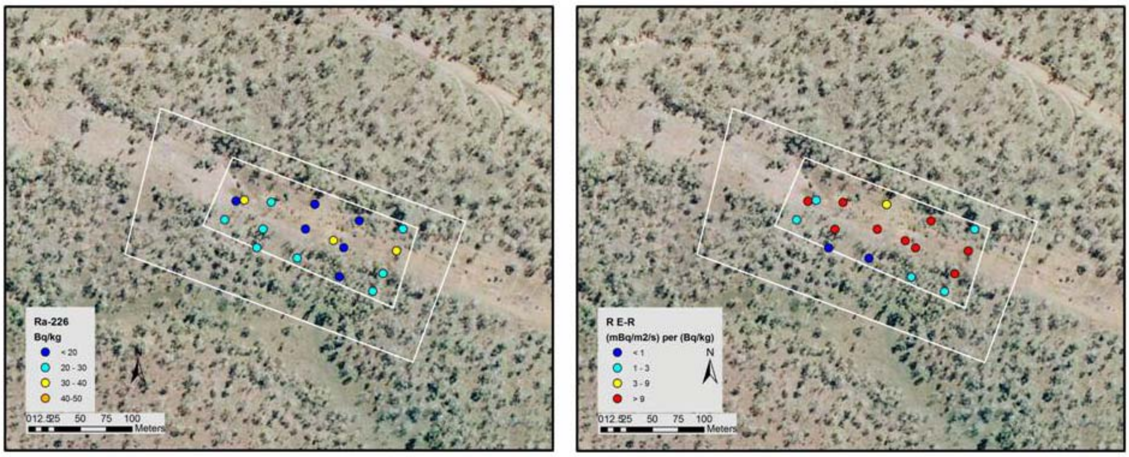

Figure 7 Soil ^{226}Ra activity concentrations [Bq·kg^{-1}] (left) and R_{E-R} [mBq·m^{-2}·s^{-1}/Bq·kg^{-1}] (right) measured at the El Sherana airstrip containment in 2012.

The variability of the ^{226}Ra soil activity concentration is low. The minimum ^{226}Ra soil activity concentration is 11 Bq·kg^{-1} and the maximum is 34 Bq·kg^{-1}. Arithmetic and geometric means are 23 and 22 Bq·kg^{-1}, respectively, with a standard deviation of 6 Bq·kg^{-1}. Results are shown in Table A4 in Appendix 4.

Saito & Jacob (1995) have used Monte Carlo methods to model the absorbed gamma dose rates 1 m above ground from measured ^{238}U, ^{232}Th and ^{40}K soil activity concentrations, assuming secular equilibrium in the ^{238}U and ^{232}Th decay chains and homogeneity of the radionuclide acitivity concentrations throughout the soil profile. The conversion equation is shown below (equation 1). Figure 8 shows a plot of the measured versus the calculated gamma dose rates for the 17 soil sampling sites.

$$H_e = a_1 \cdot {}^{238}U + a_2 \cdot {}^{232}Th + a_3 \cdot {}^{40}K \qquad (1)$$

With:

H_e: absorbed gamma dose rate 1m above ground (nGy·hr^{-1}),

a_1: 0.462 (nGy·hr^{-1})/(Bq·kg^{-1}),

a_2: 0.604 (nGy·hr^{-1})/(Bq.kg^{-1}) ,

a_3: 0.0417 (nGy·hr^{-1})/(Bq·kg^{-1}),

^{238}U, ^{232}Th, $\cdot{}^{40}K$: soil activity concentrations (Bq·kg^{-1}).

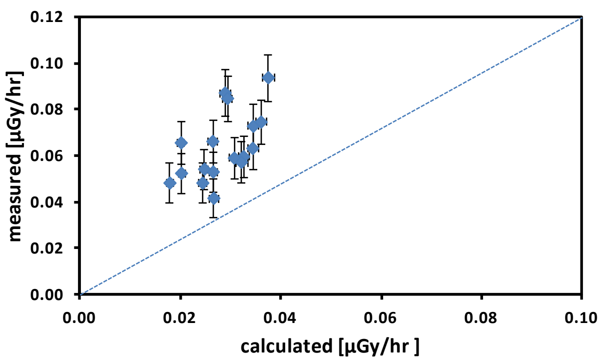

Figure 8 Measured versus calculated gamma dose rates [µGy·hr^{-1}] at the 17 soil sampling sites.

Figure 8 shows that the measured gamma dose rates are generally about two times higher than the calculated gamma dose rates, assuming that the measured soil radionuclide activity concentrations in the top 5 cm of the soils are representative for the entire soil profile. The gamma signal measured in air originates from radionuclides located in the top 0.5 m of the soil, while deeper lying radionuclides only contribute a few percent or less (depending on photon energy) to the signal (ICRU 1994; Saito & Jacob 1995). It is thus unlikely that the higher than expected gamma signal originates from the buried waste, as it is covered by more than two metres of 'clean' material. More likely, radionuclide acitivity concentrations of the containment cover below 5 cm are somewhat higher than radionuclide acitivity concentrations measured in the top 5 cm of the soil profile.

Porstendörfer (1994) discusses the theory of radon exhalation and provides a method to estimate the ^{222}Rn activity flux density E. E can be determined from the emanation power ε of radon from soil grains (which gives a value for the fraction of radon escaping from a soil grain after decay of ^{226}Ra within the grain, and is between 0 and 1), the measured soil ^{226}Ra activity concentration R [Bq·kg^{-1}], the soil density ρ [kg·m^{-3}], the ^{222}Rn decay constant λ [s^{-1}] and the ^{222}Rn diffusion length L [m^{-1}] as:

$$E = \varepsilon \cdot R \cdot \rho \cdot \lambda \cdot L \qquad (2)$$

The underlying assumptions are that flow of radon in the soil is by molecular diffusion alone, that the soil ^{226}Ra activity concentration is homogenous across the soil profile and that radon gas activity concentration at the surface of the soil can be neglected.

The typical diffusion length of ^{222}Rn in natural soils is 1.5 m (Porstendörfer 1994), the emanation power for sandy and silty loams is approximately 0.2–0.25 (Sisigina 1974), the average soil ^{226}Ra activity concentration of soils around the containment is 23 Bq·kg^{-1} (determined from soil samples taken above the containment), soil density at the containment is 1500–1600 kg·m^{-3} (O'Kane 2012) and the ^{222}Rn decay constant λ is 2.1×10^{-6} s^{-1}. With these parameters, it can be estimated that the natural background ^{222}Rn activity flux density in the area should be 20–30 mBq·m^{-2}·s^{-1}, which is in agreement with our measurements. ^{222}Rn activity flux densities measured above the containment however are much higher.

The ratio ($R_{E\text{-}R}$) has been determined of the ^{222}Rn activity flux density (mBq·m^{-2}·s^{-1}) to the measured soil ^{226}Ra activity concentration (Bqkg $^{-1}$) (Figure 7 (right) and Table A4). It has previously been shown that sites with similar geomorphologic structure and vegetation in the Alligator Rivers Region have comparable $R_{E\text{-}R}$ values and the values reported are between 0.61 (mBq·m^{-2}·s^{-1})/(Bq·kg^{-1}) for vegetated woodland and rehabilitated areas up to 2.7 (mBq·m^{-2}·s^{-1})/(Bq·kg^{-1}) for non-compacted fine grains (Lawrence et al 2009). Using equation (1) above gives typical values for natural soils of ~ 1 (mBq·m^{-2}·s^{-1})/(Bq·kg^{-1}).

Figure 7 (right) shows that most of the $R_{E\text{-}R}$ values determined for the containment are above 9 with a maximum of 41 (mBq·m^{-2}·s^{-1})/(Bq·kg^{-1}). This means that ^{222}Rn exhalation is elevated in places despite low surface soil ^{226}Ra activity concentration and similar geomorphic structure across the containment. This suggests that the elevated ^{222}Rn activity flux densities measured on top of the containment are associated with ^{222}Rn emanating from deeper sections with higher ^{226}Ra activity concentrations, diffusing through the containment cover and exhaling at the containment surface. While some of the elevated ^{222}Rn activity flux density may be due to higher ^{226}Ra activity concentrations in the cover itself, it is unlikely that this will lead to an increase of the ^{222}Rn exhalation by a factor of 40, given that measured gamma dose rates 1 m above ground are only about 2 times higher than the gamma dose rates expected from the surface soil activity concentrations.

The diffusion length L can be used to estimate the effectiveness of the cover in retaining ^{222}Rn from the buried material above which the compacted clay layer and growth medium have been placed as capping. Assuming the ^{222}Rn activity flux density from the buried material is E_0 and a layer thickness t is placed over the waste, then the ^{222}Rn activity flux density above that layer originating from the buried waste can be approximated as:

$$E = E_0 \cdot e^{-t/L} \qquad (3)$$

and the fraction reaching the surface is:

$$E/E_0 \cdot = e^{-t/L} \qquad (4)$$

Assuming an average diffusion length of 1.5 m (Porstendörfer 1994) and using a maximum thickness of the cover of 2.9 m (including the compacted clay layer) (O'Kane Consultants 2012) this fraction is about 15 % for the containment. In other words, about 15% of the ^{222}Rn emanating from the buried waste may still be exhaling at the containment surface.

Figures 3, 4 and 5 show that ^{222}Rn exhalation at the containment surface has increased between 2010 and 2012. It is important to note that the diffusion length of a material can change with factors such as soil porosity and moisture content. The effect of water content can be quite significant, particularly in the wet and dry tropics (Lawrence et al 2009), where the ground wetness can change substantially with time.

The compacted clay layer was kept moist when it was placed over the buried waste in 2009 and was then subsequently covered with topsoil. Drying and cracking of this clay layer may have occurred over the subsequent two dry seasons, and ^{222}Rn exhalation over the buried waste increased as an effect of the cracking. In addition, the establishment of vegetation on the containment and roots penetrating into the topsoil may have led to preferential pathways for ^{222}Rn to escape from deeper sections of the containment.

Equations 2 and 4 can be used to provide an estimate of the ^{226}Ra activity concentration of the buried waste. Assuming that 15% of the ^{222}Rn exhaled from the waste reaches the surface of the containment leads to ^{222}Rn activity flux densities from the waste between 70 $mBq\cdot m^{-2}\cdot s^{-1}$ (population 1 in Figure 6) and 2500 $mBq\cdot m^{-2}\cdot s^{-1}$ (for population 2 in Figure 6), respectively. Assuming a ^{222}Rn emanation coefficient between 0.07 (dry uranium ore) and 0.3 (moist uranium tailings) (Strong & Levins 1981) and using equation 2 above leads to ^{226}Ra activity concentrations of the buried waste between 50 and 7500 $Bq\cdot kg^{-1}$.

4 Dose assessment

4.1 Scenario 1: Park Rangers working on site

Parks Australia staff and Rangers have been consulted regarding person working hours on and around the El Sherana containment. The result of the consultation is that Park Rangers would spend a total of 80 person hours on site per year. Works conducted on site include general maintenance, weed and fire management and monitoring, including downloading of in-situ monitoring equipment. In our assessment it is assumed that one Ranger conducts all the work activities over one year and that the site is accessed during normal working hours.

4.1.1 External gamma dose rate

A normal probability frequency distribution plot of the above baseline gamma dose rates within the fenced area of the containment is shown in Figure 2. This plot shows that in 2012 95% of the gamma dose rates measured at the containment were less than 0.021 $\mu Gy \cdot hr^{-1}$ (lower bound: 0.019 $\mu Gy \cdot hr^{-1}$, upper bound: 0.024 $\mu Gy \cdot hr^{-1}$) and 99% were less than 0.03 $\mu Gy \cdot hr^{-1}$ (lower bound: 0.026 $\mu Gy \cdot hr^{-1}$; upper bound 0.033 $\mu Gy \cdot hr^{-1}$) above the 2007 baseline.

The 99th percentile (0.03 $\mu Gy \cdot hr^{-1}$) has been chosen as the assessment input for above baseline external gamma dose rates at the containment. Only one percent of the area on top of the containment will exhibit gamma dose rates greater than 0.03 $\mu Gy \cdot hr^{-1}$ above the baseline. A Ranger accessing the fenced site for routine work activites for 80 hours in a year would thus receive an above background annual external gamma dose below 3 µSv per year from external gamma radiation.

4.1.2 Radon decay product inhalation modelling

The radon inhalation pathway has been modelled using the computer code RESRAD-Offsite (version 2.6), developed by the Argonne National Laboratory (ANL) (Yu et al, 2009). RESRAD is a computer model designed to estimate radiation doses and risks from RESidual RADioactive materials.

RESRAD-Offsite models atmospheric transport and calculates annual doses received from the inhalation of radon decay products in air on and off-site, emitted from buried radioactive waste that is capped with a ‘clean’ cover. RESRAD-Offsite also calculates the ratio of the average airborne ^{222}Rn activity concentrations on top of the containment or downwind of the buried waste to the ^{222}Rn activity flux ($Bq \cdot s^{-1}$) exhaling from the surface of a containment, the so-called Chi over Q value ($Bq\ m^{-3}/Bq\ s^{-1}$). As the ^{222}Rn activity flux density from the containment has been determined experimentally and the containment dimensions are known (~4800 m^2), average downwind ^{222}Rn concentrations can be modelled. The 99th percentile of the ^{222}Rn activity flux density of population 2 (Figure 6) of 900 $mBqm^{-2} \cdot s^{-1}$ has been chosen for the whole containment to determine maximum ^{222}Rn activity concentrations in air, both on and off-site.

RESRAD-Offsite models annual doses from the inhalation of radon decay products from the assumed activity concentration of the buried waste, the physical properties of the waste and the cover material and meteorological parameters for the site. Default or site-specific values can be input into the program.

The parameter values chosen for the containment are shown in Table 2. It was assumed that meteorological conditions are generally stable (Pasquill stability class F; Pasquill (1974)) with the wind blowing steadily at 0.89 $m\ s^{-1}$ from the NE-NNE to the SW-SSW towards the southwestern corner of the containment. These weather conditions are unrealistic to prevail all year around and will lead to higher average ^{222}Rn activity concentrations and thus higher annual inhalation doses both on top and at the SW corner of the containment. Higher wind speeds are generally encountered and the atmospheric stability is much smaller especially during the day when the ground is heated and atmospheric convection is much larger. These daytime conditions lead to lower ^{222}Rn activity concentrations, which will generally be indistinguishable from the general background ^{222}Rn activity concentration (see for example Bollhöfer et al 2012). The parameter values in Table 2 have been chosen to determine the maximum waste origin radon decay product inhalation doses that could potentially be received on top of the containment, and results from the modelling are shown in Figure 9.

Table 2 Parameter values used for ResRad-Offsite modelling.

Parameter	**Value**	**Comment**
^{226}Ra (and ^{238}U + progeny)	18 Bq·g^{-1}	Calculated using 99th percentile Rn activity flux density and equations 2 and 4
Thickness of contaminated material	4.5 m	O'Kane (2012)
^{222}Rn diffusion coefficient of contaminated material	$5{\cdot}10^{-6}$ m^2·s^{-1}	Porstendörfer (1993)
Thickness of clean cover	1.8 m	O'Kane (2012), worst case
^{222}Rn diffusion coefficient of cover	$5{\cdot}10^{-6}$ m^2·s^{-1} (1.7-15)$\cdot10^{-6}$ m^2·s^{-1}	Porstendörfer (1993)
^{222}Rn emanation power	0.15	Strong & Levins (1981)
volumetric water content	0.01	
Wind speed	0.89 m·s^{-1}	assuming stable conditions
Wind direction	NNE-SSW (50%) and NE-SW (50%)	
Occupancy	100% outdoors	

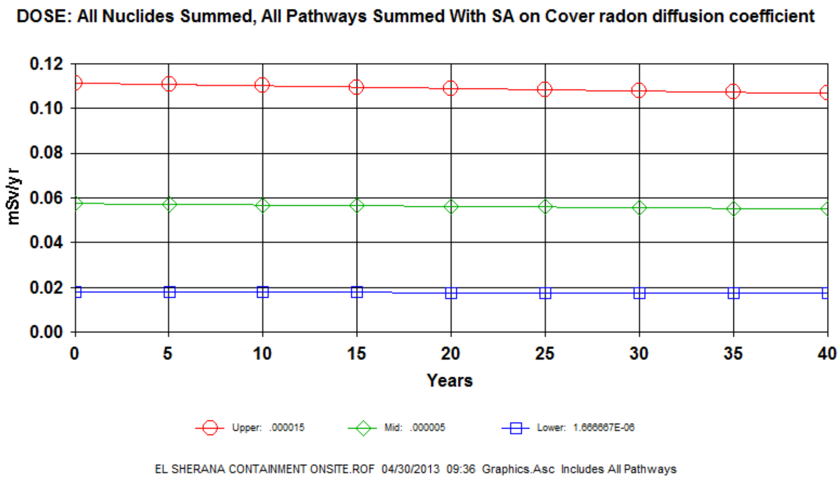

Figure 9 Annual on-site dose from the inhalation of ^{222}Rn decay products assuming access for 8760 hours per year. A sensitivity analysis of the cover ^{222}Rn diffusion coefficient has been conducted and values varied over one order of magnitude from $1.7{\times}10^{-6}$ m^2·s^{-1} (blue symbols) to $15{\times}10^{-6}$ m^2·s^{-1} (red symbols).

A sensitivity analysis has been also run on the cover ^{222}Rn diffusion coefficient, which was varied from $1.7{\times}10^{-6}$ m^2·s^{-1} to $15{\times}10^{-6}$ m^2·s^{-1}. The maximum dose from the inhalation of waste origin radon decay products on top of the containment as modelled from RESRAD-Offsite is about 0.11 mSv for 8760 hours access, or about 1 µSv if the site was accessed for 80 hours per year for general maintenance activities.

4.1.3 Dust inhalation

This pathway has not been considered as the waste is contained and covered by a cover with activity concentrations of ^{226}Ra and other radionuclides typical for background soil activity concentrations in the region. No scenario was included that assumed that the containment cover was breached (accidentally or intentionally) and the buried waste exposed during maintenance activities such as patching up of erosion channels.

4.1.4 Ingestion

The ingestion pathway has not been considered, as no bushfood items or water is consumed by Rangers in the area.

4.2 Scenario 2: Tourists visiting the area

It was assumed that tourists visit the South Alligator River valley twice in a year to access a popular camping area at Koolpin Gorge, are caught out by darkness and camp illegally at the southwest corner of the fenced area of the containment. Although there are 'better' illegal camping spots in the area, this spot is easily accessible and out of view from the gravel road to Guratba. It is also assumed that access to this area is for 10 hours during night and the early morning hours only, and that the area is accessed for camping twice, on the way in and out of the Koolpin (or other) areas. This results in 40 hours occupancy per year. The area that was assumed to be accessed for camping is shown in Figure 10, and is bordering the south western fence line.

4.2.1 External Gamma dose rate

Tourists camping outside the fence would not receive an above baseline gamma dose rate, due to their distance to the buried waste and the miniscule above background gamma dose rates at the containment.

4.2.2 Radon decay product inhalation modelling

The inputs chosen to model off-site ^{222}Rn inhalation doses are identical to the on-site scenario and are shown in Table 2.

Figure 10 shows the site set-up chosen for the overnight camping scenario. It was assumed that people camp immediately next to the fenceline. RESRAD-Offsite uses a Gaussian dispersion model to model off-site atmospheric transport and calculates annual doses received from the inhalation of radon decay products in air, emitted from buried radioactive waste that is covered with a 'clean' cover. The radon decay product inhalation doses next to the fence calculated by RESRAD-Offsite (in mSv per year) are shown in Figure 11.

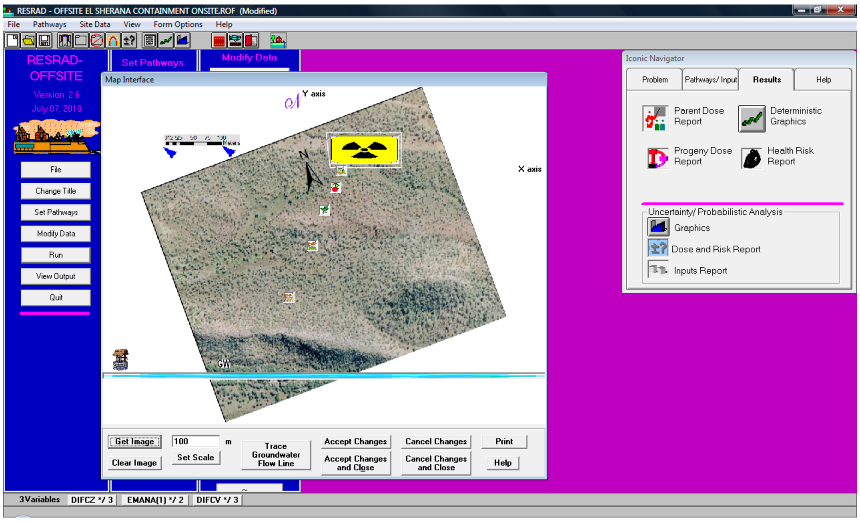

Figure 10 Site layout chosen for modelling the atmospheric pathway using ResRad-Offsite (version 2.6).

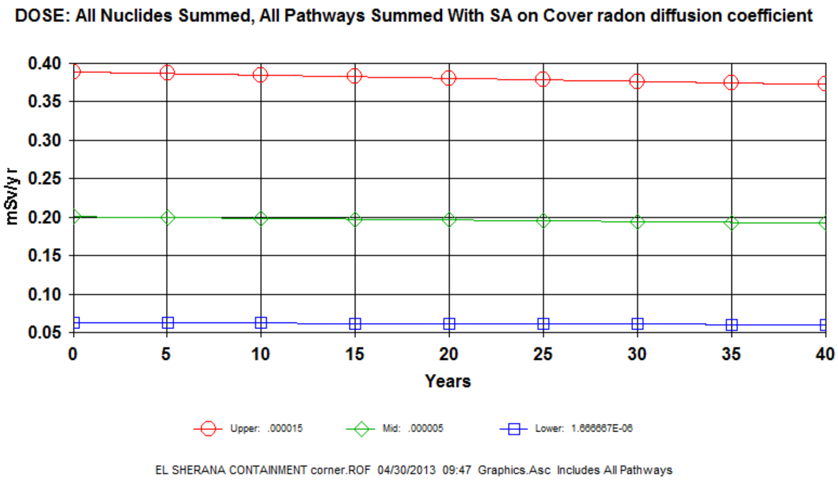

Figure 11 Maximum annual off-site dose (SW corner of containment) from the inhalation of ^{222}Rn decay products assuming access for 8760 hours per year. A sensitivity analysis of the cover ^{222}Rn diffusion coefficient has been conducted, values varied from 1.7×10^{-6} $m^2 \cdot s^{-1}$ (blue symbols) to 15×10^{-6} $m^2 \cdot s^{-1}$ (red symbols).

The Chi over Q value (Bq m^{-3}/Bq s^{-1}) can be used to calculate the waste origin airborne ^{222}Rn activity concentrations downwind of the containment. A maximum average ^{222}Rn activity flux density of 900 mBqm $^{-2} \cdot s^{-1}$ (99th percentile of population 2 in Figure 6) has been chosen to determine a maximum ^{222}Rn flux from the buried waste at the containment to 4320 Bq s^{-1}. This value and the modelled Chi over Q values have been used to determine ^{222}Rn activity concentrations in air both on and off-site from the containment (Table 3).

^{222}Rn activity concentrations in air have also been calculated for various other locations downwind of the containment, and these locations are indicated in Figure 10 as well. The distances from the containment fence were 0, 30, 75, 140 and 240 m, respectively. Figure 12 shows the ^{222}Rn activity concentration in air with distance from the location of the fence. Appendix 5 shows the RESRAD-Offsite plots (in mSv per year) for those additional offsite locations.

Table 3 Chi/Q and calculated ^{222}Rn activity and ^{222}Rn decay product (RDP) potential alpha energy concentrations.

Location of 'dwelling'	Chi/Q [s·m⁻³]	Rn [Bq·m⁻³]	RDP [µJ·m⁻³]
On Site	1.87E-03	8.1	0.0045
SW fence corner	1.30E-02	56	0.126
30 m SW of corner	2.62E-03	11	0.025
75 m SW of corner	4.90E-04	2.1	0.005
140 m SW of corner	8.31E-05	0.36	0.0008
240 m SW of corner	0.00E+00	0	0

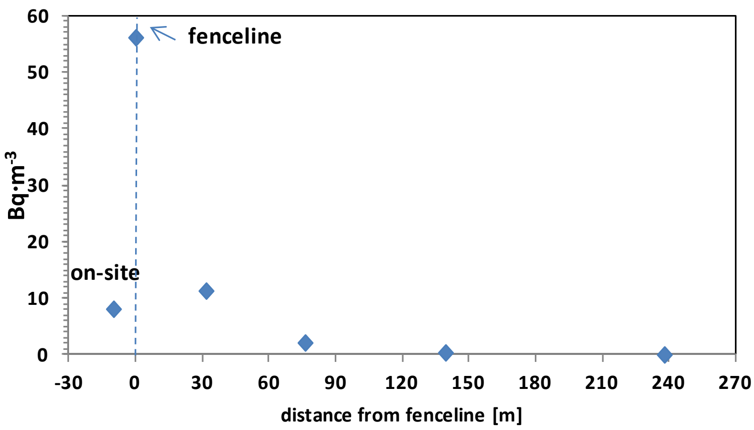

Figure 12 Waste origin ^{222}Rn concentration in air with distance from the fenceline.

The ^{222}Rn activity concentrations shown in Figure 12 have been used to determine ^{222}Rn decay product (RDP) inhalation doses for comparison with the results obtained directly from the RESRAD-Offsite modelling (Appendix 5). For this, an equilibrium factor of 0.1 (on-site) and 0.4 (off-site) has been used. These are similar to equilibrium factors determined elsewhere in the Alligator Rivers Region and the wet-dry tropics of northern Australia (Akber & Pfitzner 1994; Bollhöfer et al 2012). A conversion factor of 0.0056 µJ·Bq $^{-1}$ has been used to determine the potential alpha energy concentration of radon in equilibrium with its progeny and calculated radon decay product potential alpha energy concentration values are given in Table 3. The current ICRP recommended dose conversion coefficient for ^{222}Rn progeny for the public of 1.1 µSv per µJ·h·m^{-3} (ICRP 1993) has been used to calculate inhalation doses shown in Figure 13.

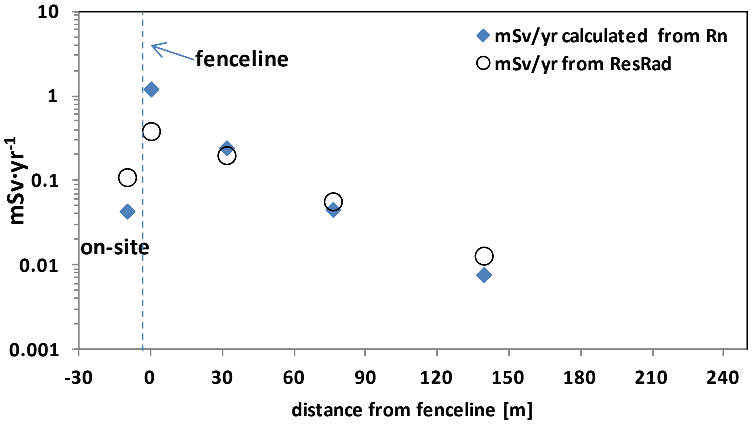

Figure 13 Waste origin ^{222}Rn decay product inhalation doses (assuming full year occupancy) plotted against distance from the fenceline. Calculated using ^{222}Rn concentrations in air from Figure 11 (blue diamonds), and modelled using ResRad-Offsite (open circles) with parameter values given in Table 2. Note the log-scale of the y-axis.

Figure 13 shows that the maximum annual ^{222}Rn decay product inhalation doses modelled from the input parameters in RESRAD-Offsite, and calculated using the Chi over Q values and maximum ^{222}Rn flux densities from the containment agree well, although the inhalation dose is somewhat higher at the fenceline when calculated using the Chi over Q values. Assuming that people camp at this spot for 40 hours total per year, will lead to a waste origin inhalation dose of approximately 6 µSv. The inhalation dose for 40 hours annual habitation is insignificant (< 0.04 µSv) at a distance of 140 m from the fenceline.

4.2.3 Dust inhalation

This pathway has not been considered as the waste is contained and covered by soil with activity concentrations of ^{226}Ra and other radionuclides typical for background soil activity concentrations in the region. No scenario was included that assumed that the containment cover was breached (accidentally or by intend) and the buried waste exposed during maintenance activities such as patching up of erosion channels.

4.2.4 Ingestion

The ingestion pathway has not been considered, as no bushfood items or water have been assumed to be consumed by Toursits camping in the area.

4.3 Scenario 3: Traditional Owners

An Aboriginal occupation scenario in the direct vicinity of the containment was considered unlikely. This is because Aboriginal people prefer other sites in the South Alligator River valley for hunting, fishing and overnight camping. Aboriginal people mainly go fishing around the One Lane Bridge or Callahan's Hut down stream on the South Alligator River, or at the Flying Fox Crossing and near the down stream end of South Alligator Gorge. These areas are several kilometers away from the containment.

Assuming that Aboriginal people camp along the banks of the South Alligator River will lead to negligible doses from the inhalation of ^{222}Rn decay products (see Figure 13) and doses from the exposure to above background gamma radiation will also be zero. It is unlikely that any terrestrial bushfood flora will be collected on site. Terrestrial animals (wallaby, buffalo or pig) which are consumed are unlikely able to access the containment and take up contaminants from the buried waste due to continuing maintenance of the fence around the containment. The groundwater levels are deeper than the buried waste (about 10–12 m below surface) and transport of groundwater from the containment to the South Alligator River is slow at about 4 mm per day (Puhalovich et al 2006). Consequently, the ingestion pathway for aquatic foods can be disregarded. Consequently, the Aboriginal occupation scenario has not been considered further in the assessment.

Summary and Conclusions

In the dry season 2009 a near-surface disposal facility was purpose-built at the disused El Sherana airstrip in the South Alligator River valley to hold NORM waste from legacy uranium mining and processing sites in the area.

Whereas the external gamma dose rates measured 1 m above ground in 2010 and 2012 are not substantially different from external gamma dose rates measured before containment construction, the geometric mean ^{222}Rn activity flux density has increased threefold from 18 mBq·m^{2}·s^{-1} in 2010 to 56 mBq·m^{2}·s^{-1} in 2012. It is possible that drying and subsequent cracking of the 0.5 m thick compacted clay layer, and the establishment of roots and thus preferential pathways for radon transport through the containment cover have contributed to the increase in ^{222}Rn activity flux density from the containment. It is important to continue ^{222}Rn exhalation measurements for the foreseeable future to assess whether ^{222}Rn activity flux densities increase further or stabilise to an average value similar to that measured in 2012.

In order to estimate expected maximum annual doses from the containment, two scenarios were considered. Scenario 1 was for Park Rangers that access the containment routinely as part of their general work duties for 80 hours in a year. Scenario 2 was for tourists visiting the area and using the area next to the south western fenceline at the containment as an overnight camping spot for four nights (40 hours) in a year. The 99th percentiles of the above background gamma radiation dose rate was used to determine doses from direct gamma radiation. The 99th percentile of the ^{222}Rn activity flux density measured in 2012 and the RESRAD-Offsite modelling program was used to determine doses from the inhalation of ^{222}Rn decay products on and off-site. Table 4 summarises the expected maximum annual doses for these scenarios.

Table 4 Maximum above background annual effective doses from the various pathways for 3 different scenarios.

	Direct γ	Inhalation		Ingestion	Total
		^{222}Rn decay products	Dust		
Park Rangers	3 μSv	1 μSv	0 μSv	0 μSv	4 μSv
Tourists	0 μSv	6 μSv	0 μSv	0 μSv	6 μSv
Aboriginal people	0 μSv	0 μSv	0 μSv	0 μSv	0 μSv

References

Akber RA & Pfizner JL 1994. Atmospheric concentrations of radon and radon daughters in jabiru East. Technical memorandum 45. Supervising Scientist for the Alligator Rivers Region. Australian Goverment Publishing Services, Canberra.

Bollhöfer A, Storm J, Martin P & Tims S 2005. Geographic variability in radon exhalation at a rehabilitated uranium mine in the Northern Territory, Australia. Environmental Monitoring and Assessment 114. 313-330.

Bollhöfer A, Dunn L, Pfitzner K, Ryan B, Fawcett M & Jones DR 2009. Remediation of the remnants of past uranium mining activities in the South Alligator River Valley. In eriss research summary 2007–2008. eds Jones DR & Webb A, Supervising Scientist Report 200, Supervising Scientist, Darwin NT, 206-211.

Bollhöfer A, Doering C, Fox G, Pfitzner J & Medley P 2012. Assessment of the radiological exposure pathways at Rum Jungle Creek South (Rum Jungle Lake Reserve) – Batchelor. Report prepared by the Environmental Research Institute of the Supervising Scientist for: Northern Territory Government Department of Resources. May 2012.

Director of National Parks 2006. *Annual Report 2005–06*. Director of National Parks, Canberra.

Doering C, Bollhöfer A, Ryan B, Sellwood J, Fox T & Pfitzner J 2011. Baseline and post-construction radiological conditions at El Sherana airstrip containment, South Alligator River valley, Australia. Internal Report 592, June, Supervising Scientist, Darwin.

Esparon A & Pfitzner J 2010. Visual gamma: ***eriss*** gamma analysis technical manual. Internal Report 539, December, Supervising Scientist, Darwin.

International Commission on Radiation Units and Measurements (ICRU) 1994. Gamma-ray spectrometry in the environment. ICRU Report 53.

International Commission on Radiological Protection (ICRP) 1993. Protection against radon-222 at home and at work. ICRP Publication 65, Annals of the ICRP 23(2).

Lawrence CE, Akber RA, Bollhöfer A & Martin P 2009. Radon-222 exhalation from open ground on and around a uranium mine in the wet-dry tropics. Journal of Environmental Radioactivity 100, 1–8.

Marten R 1992. Procedures for routine analysis of naturally occurring radionuclides in environmental samples by gamma-ray spectrometry with HPGe detectors. Internal report 76, Supervising Scientist for the Alligator Rivers Region, Canberra. Unpublished paper.

National Health and Medical Research Council (NHMRC) 1993. Code of practice for the near-surface disposal of radioactive waste in Australia (1992). Radiation Health Series No. 35.

O'Kane Consultants 2012. Gunlom Land Trust Area, Kakadu National Park Containment Facility for Radiologically Contaminated Materials – Record of Construction and Quality Control and Assurance Report. OKC Report No. 765/10-01 prepared for Parks Australia.

Ott WR 1995. Environmental Statistics and Data Analysis. Lewis Publishers.

Pasquill F, 1974. Atmospheric diffusion: the dispersion of windborne material from industrial and other sources. Chichester New York, E. Horwood; Halsted Press. 429 pp.

Pfitzner J 2010. ***eriss*** HPGe detector calibration. Internal Report 576, October, Supervising Scientist, Darwin. Unpublished paper.

Porstendörfer J 1994. Properties and behaviour of radon and thoron and their decay products in the air. Journal of Aerosol Science 25(2), 219–263.

Puhalovich A, Pillai M, McGovern E & Jacobsen N 2006. Groundwater Level Monitoring & Permeability Testing – Candidate Containment Sites (Gulom Radiological Materials). Draft Report for Parks Australia North prepared by EWL Sciences Pty Ltd. August 2006.

Saito K & Jacob P 1995. Gamma ray fields in the air due to sources in the ground. Radiat. Prot. Dosim. 58(1), 29-45.

Sisigina TI 1974. Assessment of Radon Emanation from the Surface of Extensive Territories. Nuclear Meteorology, Israeli Program of Scientific Translations, Jerusalem, p. 239.

Spehr W & Johnston A 1983. The measurement of radon emanation rates using activated charcoal. *Radiation Protection in Australia* 1(3), 113–116.

Strong KP & Levins DM 1982. Effect of Moisture Content on Radon Emanation from Uranium Ore and Tailings. Health Physics 42, 27-32.

Waggit P 2004. Uranium mine rehabilitation: The story of the South Alligator Valley intervention. *Journal of Environmental Radioactivity* 76, 51–66.

Yu C, Gnanapragasam E, Biwer B, Cheng JJ, Kamboj S, Klett T, Zielen A, Williams WA, Domotor S & Wallo A 2009. RESRAD-OFFSITE – A new member of the RESRAD family of codes. Radioprotection 44, 5. 659–664.

Appendix 1 Details of gamma survey instruments

Radiological Laboratory, Faculty of Science and Technology
Delivery Address: E-Block Store, QUT Gardens Point, Qld. 4000
Phone: 07 3138 2590; *Fax*: 07 3138 9079; *Email*: radlab@qut.edu.au

RADIATION MONITOR CALIBRATION CHECK

CLIENT: ERISS
ADDRESS: cnr Pederston Road and Fenton Court, Darwin International Airport 0820

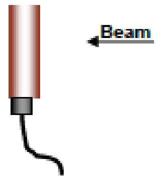

MONITOR: Mini GM Tube connected to RadEye GX
SERIAL NO: 00826

CALIBRATION SOURCE: ^{137}Cs (661.6 keV gamma emitter)
SERIAL NO.: 3702GF, Traceable to ARPANSA Air Kerma Rate Calibration, Sv/Gy = 1.21
ACTIVITY: 99.80 MBq ± 5.0% on 1/12/2012

BACKGROUND COUNT RATE: 1.8 CPS

Distance	Expected Dos Rate	Monitor Readings			Background	CPS / µSv h^{-1}	
(m)	(µSv h^{-1})	Counts	Time (s)	CPS	Corrected CPS	(%)	
0.50	42.20	59300	100	593	591	14.0	
0.75	18.76	25800	100	258	256	13.7	
1.00	10.55	15100	100	151	149	14.1	
1.25	6.75	9319	100	93.2	91.4	13.5	
1.50	4.69	6532	100	65.3	63.5	13.5	
1.75	3.44	4703	100	47.0	45.2	13.1	
2.00	2.64	3891	100	38.9	37.1	14.1	
2.50	1.69	2529	100	25.3	23.5	13.9	
3.00	1.17	1896	100	19.0	17.1	14.6	
3.50	0.86	1545	100	15.5	13.6	15.8	*
					Average	**13.8**	
					Std error	**0.2**	

COMMENTS: The average CPS per µSv h^{-1} for this detector is 13.8 ± 0.2
The reading with an * is disregarded; outside two standard deviations.

Signed: ____________________

Riaz Akber (Radioanalytical Services)

Date: 01-December-2012

Figure A1 Calibration Certificate for GM tube 2 from 1 December 2012.

Table A1 Details of instruments used to conduct the gamma dose rate measurements at the containment.

	GM1	GM2	GM3
Description	Geiger Müller tube	Geiger Müller tube	Geiger Müller tube
Manufacturer	Mini-instruments	Mini-instruments	Mini-instruments
Serial number	00827	00828	00362
Meter	RadEye GX	RadEye GX	RadEye GX
Serial number	00711	0314	00630
Correction factor[a]	0.90	1	0.86

[a] The correction factor gives the the ratio of the counts measured by the respective GM tube to the counts measured by GM tube 2 during the intercomparison in the field. Measured counts per second have been divided by this factor to correct for inter-instrument differences.

Appendix 2 Gamma dose rate measurement results

Table A2 Date, location, eastings and northings, counts per seconds and calculated absorbed gamma dose rates H_e, uncertainty in calculated dose rates and comments recorded on the fieldsheets.

Date	Location	Easting	Northing	Counts s^{-1}	+-	H_e $\mu Gy\ h^{-1}$	+-	Comments
Within fenced area								
3/09/2012	24E	228937	8506248	2.27	0.15	0.14	0.01	Off containment.
3/09/2012	25E	228931	8506232	1.98	0.14	0.12	0.01	in erosion gully (30cm deep).
3/09/2012	2E	228920	8506216	2.19	0.15	0.13	0.01	Off containment.
3/09/2012	98E	228915	8506196	2.20	0.15	0.13	0.01	Off containment.
3/09/2012	64	228904	8506167	2.12	0.15	0.13	0.01	Off containment.
3/09/2012	94	228891	8506147	2.04	0.14	0.12	0.01	Off containment.
3/09/2012	72	228865	8506161	2.21	0.15	0.13	0.01	Off containment.
3/09/2012	62E	228876	8506181	2.01	0.14	0.12	0.01	
3/09/2012	7E	228886	8506198	2.32	0.15	0.14	0.01	Next to erosion gully (~ 1m deep)
3/09/2012	70	228899	8506220	2.16	0.15	0.13	0.01	
3/09/2012	63	228905	8506241	2.09	0.14	0.13	0.01	
3/09/2012	16E	228910	8506258	2.21	0.15	0.13	0.01	Off containment.
3/09/2012	75	228876	8506265	1.93	0.14	0.12	0.01	Off containment.
3/09/2012	81	228863	8506249	1.91	0.14	0.11	0.01	
3/09/2012	79	228848	8506223	1.80	0.13	0.11	0.01	
3/09/2012	30E	228838	8506230	2.67	0.16	0.16	0.01	Weather station.
3/09/2012	83	228844	8506195	2.20	0.15	0.13	0.01	
3/09/2012	78	228833	8506170	2.13	0.15	0.13	0.01	
3/09/2012	31E	228794	8506187	2.25	0.15	0.13	0.01	
3/09/2012	10E	228803	8506213	2.56	0.16	0.15	0.01	
3/09/2012	4E	228811	8506241	1.98	0.14	0.12	0.01	
3/09/2012	90	228820	8506265	1.91	0.14	0.11	0.01	
3/09/2012	96	228824	8506289	2.49	0.16	0.15	0.01	
3/09/2012	77	228790	8506299	1.95	0.14	0.12	0.01	Off containment.
3/09/2012	35E	228778	8506267	2.52	0.16	0.15	0.01	Waypoint not saved.
3/09/2012	1E	228770	8506241	1.99	0.14	0.12	0.01	
3/09/2012	97	228764	8506223	2.06	0.14	0.12	0.01	
3/09/2012	13E	228752	8506204	2.09	0.14	0.13	0.01	Off containment.
3/09/2012	29E	228726	8506219	1.96	0.14	0.12	0.01	Off containment.
3/09/2012	20E	228733	8506250	2.10	0.14	0.13	0.01	
3/09/2012	3E	228744	8506268	2.21	0.15	0.13	0.01	
3/09/2012	17E	228752	8506269	2.35	0.15	0.14	0.01	
3/09/2012	19E	228765	8506312	2.27	0.15	0.14	0.01	Off containment.
3/09/2012	71	228722	8506323	2.13	0.15	0.13	0.01	Off containment.
3/09/2012	69	228716	8506299	2.28	0.15	0.14	0.01	Off containment.
3/09/2012	87	228709	8506272	1.95	0.14	0.12	0.01	Off containment.
3/09/2012	36E	228693	8506238	2.22	0.15	0.13	0.01	Off containment.
3/09/2012	14E	228687	8506218	2.32	0.15	0.14	0.01	Off containment.

Date	Location	Easting	Northing	Counts s^{-1}	+-	E $\mu Gy\ h^{-1}$	+-	Comments
4/09/2012		228668	8506333	2.39	0.15	0.14	0.01	
4/09/2012		228683	8506327	2.02	0.14	0.12	0.01	
4/09/2012		228702	8506321	2.05	0.14	0.12	0.01	
4/09/2012		228722	8506314	1.89	0.14	0.11	0.01	
4/09/2012		228738	8506306	2.04	0.14	0.12	0.01	
4/09/2012		228759	8506300	2.33	0.15	0.14	0.01	
4/09/2012		228774	8506294	2.30	0.15	0.14	0.01	
4/09/2012		228789	8506286	2.14	0.15	0.13	0.01	
4/09/2012		228805	8506282	2.14	0.15	0.13	0.01	
4/09/2012		228826	8506278	2.55	0.16	0.15	0.01	
4/09/2012		228844	8506270	1.92	0.14	0.11	0.01	
4/09/2012		228861	8506264	1.87	0.14	0.11	0.01	
4/09/2012		228878	8506258	2.38	0.15	0.14	0.01	
4/09/2012		228893	8506247	2.42	0.16	0.14	0.01	
4/09/2012		228910	8506241	2.02	0.14	0.12	0.01	
4/09/2012		228922	8506236	2.44	0.16	0.15	0.01	
4/09/2012		228942	8506232	2.38	0.15	0.14	0.01	
4/09/2012		228957	8506222	2.48	0.16	0.15	0.01	
4/09/2012		228936	8506171	1.97	0.14	0.12	0.01	
4/09/2012		228920	8506180	2.40	0.15	0.14	0.01	
4/09/2012		228905	8506185	2.17	0.15	0.13	0.01	
4/09/2012		228887	8506193	1.85	0.14	0.11	0.01	
4/09/2012		228883	8506193	2.21	0.15	0.13	0.01	On side of erosion gully.
4/09/2012		228877	8506188	2.14	0.15	0.13	0.01	Inside erosion gully.
4/09/2012		228869	8506203	2.06	0.14	0.12	0.01	
4/09/2012		228861	8506203	1.89	0.14	0.11	0.01	On side of erosion gully.
4/09/2012		228858	8506196	2.11	0.15	0.13	0.01	Inside erosion gully.
4/09/2012		228849	8506202	2.43	0.16	0.15	0.01	
4/09/2012		228835	8506209	2.34	0.15	0.14	0.01	
4/09/2012		228816	8506218	1.93	0.14	0.12	0.01	
4/09/2012		228800	8506224	2.27	0.15	0.14	0.01	Inside earthworks - rise on edges.
4/09/2012		228785	8506232	2.69	0.16	0.16	0.01	Next to sediment trap.
4/09/2012		228765	8506242	2.34	0.15	0.14	0.01	
4/09/2012		228749	8506247	2.39	0.15	0.14	0.01	
4/09/2012		228734	8506252	2.25	0.15	0.13	0.01	
4/09/2012		228716	8506258	1.86	0.14	0.11	0.01	
4/09/2012		228697	8506265	2.17	0.15	0.13	0.01	
4/09/2012		228682	8506273	2.16	0.15	0.13	0.01	
4/09/2012		228661	8506281	2.37	0.15	0.14	0.01	
4/09/2012		228650	8506244	2.23	0.15	0.13	0.01	
4/09/2012		228666	8506237	2.00	0.14	0.12	0.01	
4/09/2012		228683	8506233	1.80	0.13	0.11	0.01	
4/09/2012		228703	8506228	1.74	0.13	0.10	0.01	

Date	Location	Easting	Northing	Counts s^{-1}	+-	E $\mu Gy\ h^{-1}$	+-	Comments
4/09/2012		228715	8506220	2.18	0.15	0.13	0.01	
4/09/2012		228730	8506215	2.25	0.15	0.13	0.01	
4/09/2012		228739	8506209	2.16	0.15	0.13	0.01	
4/09/2012		228761	8506200	2.54	0.16	0.15	0.01	
4/09/2012		228772	8506197	2.59	0.16	0.16	0.01	
4/09/2012		228790	8506188	2.22	0.15	0.13	0.01	
4/09/2012		228807	8506183	2.10	0.14	0.13	0.01	
4/09/2012		228819	8506178	2.08	0.14	0.12	0.01	
4/09/2012		228842	8506170	2.55	0.16	0.15	0.01	Washout, bottom of erosion gully
4/09/2012		228859	8506159	2.18	0.15	0.13	0.01	
4/09/2012		228873	8506152	2.02	0.14	0.12	0.01	
4/09/2012		228897	8506148	1.98	0.14	0.12	0.01	
4/09/2012		228913	8506140	2.32	0.15	0.14	0.01	
4/09/2012		228665	8506320	2.57	0.21	0.15	0.01	West gate.
4/09/2012		228680	8506318	2.33	0.20	0.14	0.01	
4/09/2012		228698	8506310	2.33	0.20	0.14	0.01	
4/09/2012		228715	8506297	2.27	0.19	0.14	0.01	Next to radon cup.
4/09/2012		228732	8506293	2.30	0.19	0.14	0.01	At bottom of containment; west.
4/09/2012		228752	8506284	2.24	0.19	0.13	0.01	Top of containment.
4/09/2012		228768	8506284	2.28	0.19	0.14	0.01	Top of containment.
4/09/2012		228783	8506273	2.35	0.20	0.14	0.01	Top containment, close to Rn cup
4/09/2012		228798	8506266	2.45	0.20	0.15	0.01	
4/09/2012		228816	8506261	2.17	0.19	0.13	0.01	Weather station.
4/09/2012		228832	8506255	2.26	0.19	0.14	0.01	
4/09/2012		228851	8506250	2.17	0.19	0.13	0.01	
4/09/2012		228866	8506244	2.05	0.18	0.12	0.01	
4/09/2012		228887	8506238	2.05	0.18	0.12	0.01	
4/09/2012		228908	8506233	2.42	0.20	0.15	0.01	Gully start. Next to east marker
4/09/2012		228924	8506221	2.18	0.19	0.13	0.01	Bottom of containment; east.
4/09/2012		228937	8506217	2.16	0.19	0.13	0.01	
4/09/2012		228948	8506206	1.94	0.18	0.12	0.01	On access track.
4/09/2012		228944	8506189	2.57	0.21	0.15	0.01	
4/09/2012		228929	8506197	2.38	0.20	0.14	0.01	
4/09/2012		228909	8506203	2.11	0.19	0.13	0.01	Bottom of containment; east.
4/09/2012		228894	8506209	2.37	0.20	0.14	0.01	Top of containment.
4/09/2012		228889	8506211	2.48	0.20	0.15	0.01	Start of erosion gully.
4/09/2012		228878	8506216	2.19	0.19	0.13	0.01	
4/09/2012		228857	8506218	1.98	0.18	0.12	0.01	
4/09/2012		228837	8506224	2.59	0.21	0.15	0.01	top of containment
4/09/2012		228833	8506235	2.12	0.19	0.13	0.01	
4/09/2012		228805	8506240	1.94	0.18	0.12	0.01	weather station.
4/09/2012		228788	8506246	2.55	0.21	0.15	0.01	
4/09/2012		228770	8506254	2.34	0.20	0.14	0.01	

Date	Location	Easting	Northing	Counts s^{-1}	+-	E $\mu Gy\ h^{-1}$	+-	Comments
4/09/2012		228761	8506265	2.40	0.20	0.14	0.01	
4/09/2012		228738	8506271	2.32	0.20	0.14	0.01	
4/09/2012		228722	8506277	2.91	0.22	0.17	0.01	Bottom of containment; west.
4/09/2012		228707	8506280	2.13	0.19	0.13	0.01	
4/09/2012		228694	8506288	1.98	0.18	0.12	0.01	
4/09/2012		228676	8506295	2.13	0.19	0.13	0.01	
4/09/2012		228661	8506300	2.32	0.20	0.14	0.01	Fence.
4/09/2012		228643	8506207	1.95	0.18	0.12	0.01	
4/09/2012		228650	8506198	2.33	0.20	0.14	0.01	
4/09/2012		228664	8506190	2.15	0.19	0.13	0.01	
4/09/2012		228688	8506184	2.39	0.20	0.14	0.01	
4/09/2012		228698	8506177	2.30	0.19	0.14	0.01	
4/09/2012		228713	8506171	1.62	0.16	0.10	0.01	
4/09/2012		228731	8506165	2.12	0.19	0.13	0.01	
4/09/2012		228744	8506155	2.05	0.18	0.12	0.01	
4/09/2012		228760	8506153	2.05	0.18	0.12	0.01	
4/09/2012		228778	8506147	2.09	0.18	0.13	0.01	
4/09/2012		228798	8506139	1.94	0.18	0.12	0.01	
4/09/2012		228808	8506132	2.25	0.19	0.13	0.01	
4/09/2012		228824	8506122	2.04	0.18	0.12	0.01	
4/09/2012		228842	8506120	2.09	0.18	0.13	0.01	
4/09/2012		228864	8506113	1.79	0.17	0.11	0.01	
4/09/2012		228885	8506105	2.09	0.18	0.13	0.01	
4/09/2012		228900	8506098	2.13	0.19	0.13	0.01	
4/09/2012		228674	8506350	2.12	0.18	0.13	0.01	
4/09/2012		228690	8506344	2.45	0.19	0.15	0.01	
4/09/2012		228707	8506338	2.22	0.18	0.13	0.01	
4/09/2012		228726	8506331	2.54	0.20	0.15	0.01	
4/09/2012		228747	8506326	2.12	0.18	0.13	0.01	
4/09/2012		228766	8506318	2.23	0.18	0.13	0.01	
4/09/2012		228782	8506311	2.16	0.18	0.13	0.01	
4/09/2012		228797	8506307	2.35	0.19	0.14	0.01	
4/09/2012		228814	8506300	2.28	0.19	0.14	0.01	
4/09/2012		228834	8506295	2.18	0.18	0.13	0.01	
4/09/2012		228851	8506288	1.98	0.17	0.12	0.01	
4/09/2012		228869	8506280	2.42	0.19	0.14	0.01	
4/09/2012		228885	8506274	2.23	0.18	0.13	0.01	
4/09/2012		228901	8506267	2.32	0.19	0.14	0.01	
4/09/2012		228916	8506262	2.47	0.20	0.15	0.01	
4/09/2012		228935	8506258	2.45	0.19	0.15	0.01	
4/09/2012		228949	8506248	2.43	0.19	0.15	0.01	
4/09/2012		228965	8506243	1.86	0.17	0.11	0.01	
4/09/2012		228929	8506153	2.13	0.18	0.13	0.01	

Date	Location	Easting	Northing	Counts s^{-1}	+-	E $\mu Gy\ h^{-1}$	+-	Comments
4/09/2012		228916	8506164	1.98	0.17	0.12	0.01	
4/09/2012		228899	8506167	2.06	0.18	0.12	0.01	
4/09/2012		228880	8506169	2.01	0.17	0.12	0.01	
4/09/2012		228873	8506178	2.39	0.19	0.14	0.01	On edge of erosion gully.
4/09/2012		228858	8506180	2.25	0.19	0.13	0.01	On edge of erosion gully.
4/09/2012		228849	8506184	2.05	0.18	0.12	0.01	On bottom of erosion gully.
4/09/2012		228841	8506187	2.36	0.19	0.14	0.01	On edge of erosion gully.
4/09/2012		228830	8506193	2.41	0.19	0.14	0.01	
4/09/2012		228807	8506198	2.18	0.18	0.13	0.01	On edge of erosion gully.
4/09/2012		228792	8506207	2.37	0.19	0.14	0.01	
4/09/2012		228778	8506217	1.85	0.17	0.11	0.01	In between two erosion gullys.
4/09/2012		228757	8506226	2.33	0.19	0.14	0.01	
4/09/2012		228742	8506230	2.32	0.19	0.14	0.01	
4/09/2012		228726	8506231	2.16	0.18	0.13	0.01	
4/09/2012		228708	8506242	2.01	0.17	0.12	0.01	
4/09/2012		228688	8506248	2.06	0.18	0.12	0.01	
4/09/2012		228669	8506253	2.22	0.18	0.13	0.01	
4/09/2012		228653	8506258	2.31	0.19	0.14	0.01	
4/09/2012		228649	8506224	2.25	0.19	0.13	0.01	
4/09/2012		228659	8506215	2.16	0.18	0.13	0.01	
4/09/2012		228674	8506209	2.03	0.17	0.12	0.01	
4/09/2012		228692	8506202	2.03	0.17	0.12	0.01	
4/09/2012		228708	8506198	2.33	0.19	0.14	0.01	
4/09/2012		228720	8506191	2.17	0.18	0.13	0.01	
4/09/2012		228736	8506184	2.19	0.18	0.13	0.01	
4/09/2012		228751	8506178	2.14	0.18	0.13	0.01	
4/09/2012		228766	8506169	1.85	0.17	0.11	0.01	
4/09/2012		228784	8506164	1.91	0.17	0.11	0.01	
4/09/2012		228800	8506155	2.25	0.19	0.13	0.01	
4/09/2012		228820	8506152	2.02	0.17	0.12	0.01	
4/09/2012		228837	8506143	2.22	0.18	0.13	0.01	
4/09/2012		228855	8506137	2.06	0.18	0.12	0.01	
4/09/2012		228873	8506131	2.17	0.18	0.13	0.01	
4/09/2012		228892	8506126	2.18	0.18	0.13	0.01	
4/09/2012		228910	8506118	2.05	0.18	0.12	0.01	
North of fenced area								
4/09/2012		228975	8506270	2.29	0.15	0.14	0.01	
4/09/2012		228948	8506280	2.71	0.16	0.16	0.01	
4/09/2012		228919	8506286	2.45	0.16	0.15	0.01	
4/09/2012		228892	8506293	2.52	0.16	0.15	0.01	
4/09/2012		228870	8506305	2.28	0.15	0.14	0.01	
4/09/2012		228845	8506315	2.27	0.15	0.14	0.01	
4/09/2012		228821	8506324	2.32	0.15	0.14	0.01	

Date	Location	Easting	Northing	Counts s^{-1}	+-	E $\mu Gy\ h^{-1}$	+-	Comments
4/09/2012		228788	8506336	1.93	0.14	0.12	0.01	
4/09/2012		228764	8506345	2.00	0.14	0.12	0.01	
4/09/2012		228747	8506351	2.24	0.15	0.13	0.01	Edge of gravel pit
4/09/2012		228719	8506342	2.17	0.15	0.13	0.01	road outside containment fence.
4/09/2012		228698	8506350	2.21	0.15	0.13	0.01	
4/09/2012		228670	8506359	2.45	0.16	0.15	0.01	
4/09/2012		228994	8506315	2.30	0.19	0.14	0.01	
4/09/2012		228964	8506316	2.64	0.21	0.16	0.01	
4/09/2012		228926	8506334	2.82	0.22	0.17	0.01	
4/09/2012		228903	8506343	2.97	0.23	0.18	0.01	
4/09/2012		228881	8506350	2.45	0.20	0.15	0.01	
4/09/2012		228857	8506358	2.69	0.21	0.16	0.01	
4/09/2012		228831	8506368	2.80	0.22	0.17	0.01	
4/09/2012		228807	8506378	2.47	0.20	0.15	0.01	
4/09/2012		228779	8506389	2.17	0.19	0.13	0.01	
4/09/2012		228755	8506392	2.49	0.20	0.15	0.01	
4/09/2012		228728	8506403	2.24	0.19	0.13	0.01	
4/09/2012		228705	8506409	2.49	0.20	0.15	0.01	
4/09/2012		228684	8506427	1.99	0.18	0.12	0.01	
4/09/2012		228987	8506291	2.23	0.18	0.13	0.01	
4/09/2012		228950	8506300	2.80	0.21	0.17	0.01	
4/09/2012		228922	8506310	2.63	0.20	0.16	0.01	
4/09/2012		228896	8506318	2.52	0.20	0.15	0.01	
4/09/2012		228881	8506326	2.60	0.20	0.16	0.01	
4/09/2012		228847	8506337	2.75	0.21	0.16	0.01	
4/09/2012		228824	8506347	2.54	0.20	0.15	0.01	
4/09/2012		228794	8506353	2.24	0.18	0.13	0.01	
4/09/2012		228772	8506364	2.24	0.18	0.13	0.01	
4/09/2012		228752	8506373	2.23	0.18	0.13	0.01	
4/09/2012		228730	8506388	2.36	0.19	0.14	0.01	
4/09/2012		228699	8506397	2.25	0.19	0.13	0.01	
4/09/2012		228681	8506403	2.29	0.19	0.14	0.01	
North of fenced area								
3/09/2012	68	228676	8506197	2.22	0.15	0.13	0.01	Outside fence.
3/09/2012	95	228729	8506175	1.93	0.14	0.12	0.01	Outside fence.
3/09/2012	8E	228769	8506147	2.19	0.15	0.13	0.01	Outside fence.
3/09/2012	18E	228823	8506110	1.94	0.14	0.12	0.01	Outside fence.
3/09/2012	40	228877	8506087	1.74	0.13	0.10	0.01	Outside fence.
4/09/2012		228856	8506086	1.98	0.18	0.12	0.01	
4/09/2012		228838	8506097	1.96	0.18	0.12	0.01	
4/09/2012		228790	8506112	1.97	0.18	0.12	0.01	
4/09/2012		228756	8506123	1.95	0.18	0.12	0.01	
4/09/2012		228731	8506124	1.96	0.18	0.12	0.01	

Date	Location	Easting	Northing	Counts s^{-1}	+-	E $\mu Gy\ h^{-1}$	+-	Comments
4/09/2012		228704	8506130	2.22	0.19	0.13	0.01	
4/09/2012		228672	8506136	1.99	0.18	0.12	0.01	
4/09/2012		228644	8506144	2.11	0.19	0.13	0.01	
4/09/2012		228627	8506148	2.47	0.20	0.15	0.01	
4/09/2012		228659	8506133	2.05	0.18	0.12	0.01	
4/09/2012		228688	8506124	2.08	0.18	0.12	0.01	
4/09/2012		228716	8506118	2.12	0.19	0.13	0.01	
4/09/2012		228749	8506108	1.93	0.18	0.12	0.01	
4/09/2012		228780	8506098	1.75	0.17	0.10	0.01	
4/09/2012		228809	8506081	2.17	0.19	0.13	0.01	
4/09/2012		228840	8506071	1.98	0.18	0.12	0.01	
4/09/2012		228868	8506052	2.01	0.18	0.12	0.01	
4/09/2012		228895	8506038	2.03	0.18	0.12	0.01	
4/09/2012		228620	8506125	2.01	0.17	0.12	0.01	
4/09/2012		228653	8506114	1.73	0.16	0.10	0.01	
4/09/2012		228684	8506103	2.19	0.18	0.13	0.01	
4/09/2012		228715	8506092	2.12	0.18	0.13	0.01	
4/09/2012		228749	8506083	2.19	0.18	0.13	0.01	
4/09/2012		228773	8506071	1.92	0.17	0.11	0.01	
4/09/2012		228804	8506054	2.10	0.18	0.13	0.01	
4/09/2012		228834	8506042	2.34	0.19	0.14	0.01	
4/09/2012		228862	8506031	1.92	0.17	0.11	0.01	
4/09/2012		228893	8506019	2.13	0.18	0.13	0.01	

Appendix 3 ^{222}Rn activity flux density measurement results

Table A3 Canister number, eastings and northings, ^{222}Rn activity flux density and comments recorded on fieldsheets.

Canister	Easting	Northing	Rn [mBq m^{-2} s^{-1}]	Comments
1E	228770	8506241	326±7	
24E	228937	8506248	24±2	Off containment.
25E	228931	8506232	21±2	Off containment; in an erosion gully (30cm deep).
30E	228838	8506230	419±8	Weather station.
31E	228794	8506187	33±2	off containment
36E	228693	8506238	41±2	Off containment.
3E	228744	8506268	241±5	
40	228877	8506087	28±2	Outside containment fence.
4E	228811	8506241	415±8	
62E	228876	8506181	24±2	
63	228905	8506241	34±2	
64	228904	8506167	30±2	Off containment.
70	228899	8506220	443±8	
71	228722	8506323	54±3	Off containment.
77	228790	8506299	33±2	Off containment.
78	228833	8506170	24±2	off containment
79	228848	8506223	745±12	
20E	228733	8506250	30±2	
69	228716	8506299	47±2	Off containment.
35E	228778	8506267	570±9	Waypoint not saved.
10E	228803	8506213	20±2	
14E	228687	8506218	43±2	Off containment.
16E	228910	8506258	20±2	Off containment.
17E	228752	8506269	42±2	
8E	228823	8506110	9±2	Outside containment fence.
19E	228765	8506312	37±2	Off containment.
29E	228726	8506219	32±2	Off containment.
2E	228920	8506216	31±2	Off containment.
68	228676	8506197	25±2	Outside containment fence.
72	228865	8506161	22±2	Off containment.
75	228876	8506265	24±2	Off containment.
7E	228886	8506198	342±7	Next to a deep erosion gully (Approx. 1m deep)
81	228863	8506249	263±6	
83	228844	8506195	27±2	
87	228709	8506272	31±2	Off containment.
8E	228769	8506147	30±2	Outside containment fence.

90	228820	8506265	111±4	
13E	228752	8506204	27±2	Off containment.
Canister	**Easting**	**Northing**	**Rn [mBq m^{-2} s^{-1}]**	**Comments**
94	228891	8506147	28±2	Off containment.
95	228729	8506175	22±2	Outside containment fence.
96	228824	8506289	19±2	Off containment.
97	228764	8506223	18±2	
98E	228915	8506196	26±2	Off containment.

Appendix 4 Soil activity concentration measurement results

Table A4 Results of soil radionuclide activity concentration measurements for 17 radon exhalation measurement sites (canister numbers), radon flux densities and $R_{E\text{-}R}$ ($mBq \cdot m^{-2} \cdot s^{-1}$ per $Bq \cdot kg^{-1}$).

SampleCode	Can	^{238}U [$Bq \cdot kg^{-1}$]	^{226}Ra [$Bq \cdot kg^{-1}$]	^{228}Ra- [$Bq \cdot kg^{-1}$]	^{228}Th [$Bq \cdot kg^{-1}$]	^{40}K [$Bq \cdot kg^{-1}$]	^{222}Rn [$mBq \cdot m^{-2} \cdot s^{-1}$]	$R_{E\text{-}R}$
XX12057	1E	14±3	22.5±0.3	17.1±0.5	17.0±0.5	138±4	326±7	14.5±0.4
XX12058	3E	18±4	19.2±0.3	16.1±0.5	18.0±0.5	158±4	241±5	12.6±0.4
XX12059	4E	14±3	17.9±0.3	12.1±0.4	13.2±0.4	93±3	415±8	23.3±0.6
XX12062	7E	20±4	25.0±0.4	20.4±0.6	23.3±0.6	209±5	342±7	13.7±0.3
XX12063	10E	15±3	21.4±0.3	18.1±0.5	19.4±0.5	172±4	20±2	0.9±0.1
XX12064	17E	23±4	33.0±0.4	18.5±0.6	19.9±0.5	209±5	42±2	1.3±0.1
XX12066	20E	33±4	26.5±0.4	18.1±0.5	20.7±0.5	184±4	30±2	1.1±0.1
XX12067	30E	24±3	34.0±0.4	18.9±0.5	20.5±0.5	222±5	419±8	12.3±0.3
XX12068	35E	25±4	25.5±0.4	17.1±±0.5	18.7±0.5	149±4	570±9	22.4±0.5
XX12072	62E	26±3	20.6±0.3	16.6±0.5	16.9±0.5	119±3	24±2	1.2±0.1
XX12060	63	34±4	24.9±0.4	18.6±0.6	19.1±0.5	181±4	34±2	1.4±0.1
XX12061	70	8±3	30.5±0.4	19.3±0.5	20.3±0.5	191±4	443±8	14.5±0.3
XX12065	79	29±4	18.4±0.3	17.4±0.5	18.8±0.5	160±4	745±12	40.5±0.9
XX12069	81	15±3	11.0±0.2	11.3±0.4	12.5±0.4	80±3	263±6	23.9±0.7
XX12070	83	14±3	18.3±0.3	12.3±0.4	13.4±0.4	83±3	27±2	1.5±0.1
XX12071	90	14±3	19.5±0.3	15.3±0.5	15.1±0.4	150±4	111±4	5.7±0.2
XX12073	97	32±4	20.3±0.3	19.0±0.6	21.7±0.6	228±5	18±2	0.9±0.1

Appendix 5 Results from ResRad-Offsite modelling

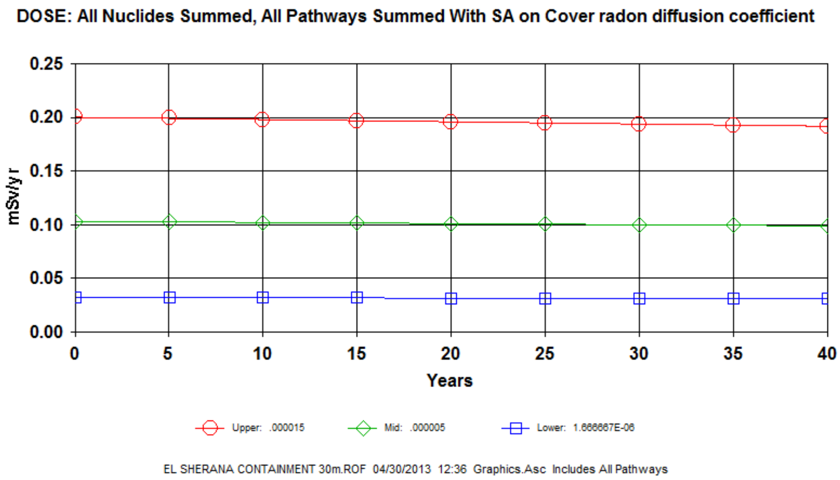

Figure A5.1 Maximum annual doses [mSv·yr-1] received from the inhalation of radon decay products from 0-40 years, 30 m downwind of the El Sherana containment.

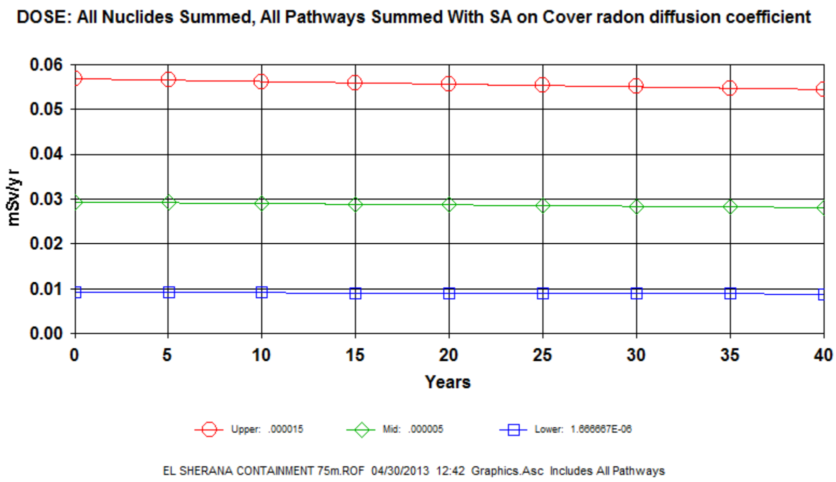

Figure A5.2 Maximum annual doses [mSv·yr-1] received from the inhalation of radon decay products from 0-40 years, 75 m downwind of the El Sherana containment.

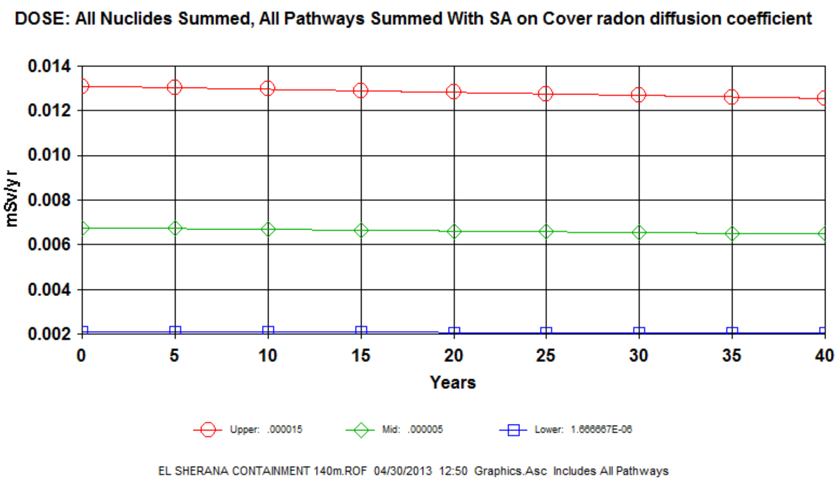

Figure A5.3 Maximum annual doses [$mSv \cdot yr^{-1}$] received from the inhalation of radon decay products from 0-40 years, 140 m downwind of the El Sherana containment.

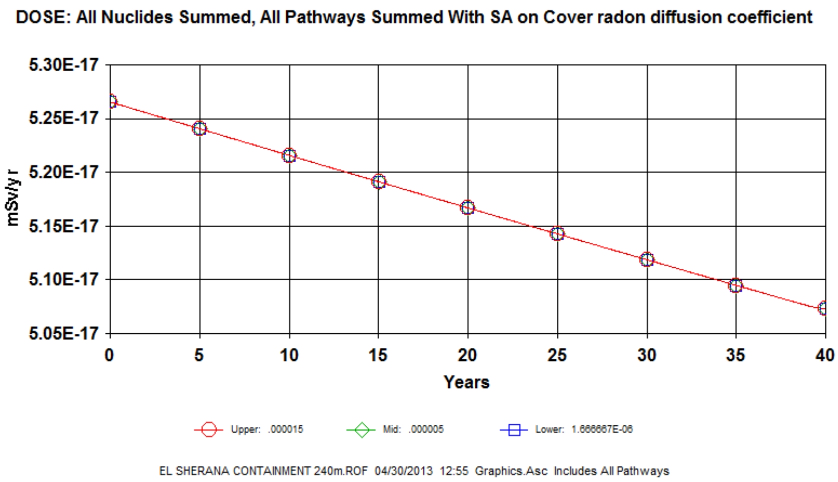

Figure A5.4 Maximum annual doses [$mSv \cdot yr^{-1}$] received from the inhalation of radon decay products from 0-40 years, 240 m downwind of the El Sherana containment.

Appendix 6 Report provided to Parks Australia, May 2013

Expected maximum doses to the public from the El Sherana airstrip containment

Andreas Bollhöfer & Che Doering

Environmental Research Institute of the Supervising Scientist, Darwin. May 2013

1 Introduction

1.1 Background

The El Sherana airstrip containment is a near-surface disposal facility located in the South Alligator Valley area in the south of Kakadu National Park. It contains approximately 22,000 m^3 of contaminated waste from historic uranium mining activities conducted in the area between 1955 and 1964. It was built as part of a lease agreement between the Gunlom Aboriginal Land Trust and the Director of National Parks for traditional Aboriginal lands in the upper South Alligator Valley to be managed as part of Kakadu National Park.

The containment was constructed, filled and covered in the 2009 dry season. It is currently in the institutional control period. This is the period following closure of the facility during which public access to, or alternative use of, the site must be restricted (NHMRC 1993). A boundary fence and warning signs are in place at the containment to restrict access and deter against alternative uses of the site, including camping.

The containment is currently managed by Parks Australia with regulatory oversight by the Australian Radiation Protection and Nuclear Safety Agency (ARPANSA). An inspection of Parks Australia by ARPANSA on 27–28 September 2011 highlighted that dose constraints for the containment had not been established. The inspection report (ARPANSA 2011) recommended that:

"Parks Australia should undertake an updated assessment of the impact of the containment taking account of recently acquired monitoring data. Once levels are proposed, ARPANSA will agree on dose constraint levels with Parks Australia."

Parks Australia subsequently requested the assistance of the Supervising Scientist Division (SSD) to help address this recommendation. In particular, it was requested that SSD conduct an assessment of potential doses to workers and the public from the containment that could be used to guide decision making on dose constraints.

1.2 Objective

The objective of this report is to summarise the results of an assessment of expected maximum doses to workers and the public from the El Sherana airstrip containment (Bollhöfer et al 2013) that can be used by Parks Australia to propose dose constraints to ARPANSA for the containment.

1.3 Scope

The assessment applies to the current radiological conditions of the containment and for its normal (passive) operation. No breach of the surface cover of the containment, either intentionally or by natural processes, was assumed in the assessment.

2 Method

2.1 Exposure scenarios

2.1.1 Occupational

It was assumed that a Park Ranger spends 80 hours per year working onsite at the containment. Work conducted at the site was assumed to include general site maintenance, weed and fire management and downloading in-situ monitoring equipment. Digging into the buried waste or repair of the capping layer or surface cover was not considered in the assessment, as this was not considered to be part of the normal (passive) operation of the containment.

2.1.2 Public (tourist camping)

It was assumed that a tourist camped for four nights (40 hours in total) next to the boundary fence of the containment. The camping location was assumed to be immediately downwind of the containment to give the highest possible exposure scenario. No inadvertent or intentional intrusion of the fence was assumed.

2.1.3 Public (Aboriginal person)

An exposure scenario for Aboriginal people was not assessed, as anecdotal evidence suggested that they do not spend time in the immediate vicinity of the containment, but rather prefer other sites in the South Alligator Valley for hunting, fishing and camping. The likelihood of exposure of an Aboriginal person was considered negligible.

2.2 Exposure pathways

Table 1 gives the exposure pathways included in the assessment for each exposure scenario. For the occupational scenario, the pathways included were radon progeny inhalation and external gamma radiation. For the public (tourist camping) scenario, the only pathway included was radon progeny inhalation. The dust inhalation pathway was not included in either scenario as the contaminated waste was assumed to be permanently buried under a clay capping layer and clean soil cover, with no breach of the capping layer. Any radionuclides in dust from the soil cover were considered to be part of the natural background.

The ingestion pathway was not included as bushfoods and locally sourced water were not considered to be consumed in either the occupational or public exposure scenario. Additionally, it is unlikely that any terrestrial plant-based bushfood would be collected onsite by the public, nor is it likely that terrestrial animals (such as wallaby, pig or buffalo) that are sometimes consumed by Aboriginal people would be able to access the site and take up radionuclides from the buried waste due to the presence of the boundary fence during the institutional control period. Groundwater levels are deeper than the buried waste (10-12 m below surface) and transport of groundwater from the containment to the South Alligator River is slow (~ 4 mm/day) (Puhalovich et al 2006) and consequently the ingestion pathway for aquatic bushfoods and water is negligible, at least for the institutional control period.

Table 1. Exposure pathways considered in the assessment of each exposure scenario[1].

	External gamma	Radon progeny	Dust	Ingestion
Occupational	✓	✓	n.a.	n.a.
Public	n.a.	✓	n.a.	n.a.

[1]n.a. = not applicable.

2.3 Radiological characteristics

SSD has made measurements of external gamma dose rates and radon exhalation flux densities at the containment at the following points in time:

- 2007 and 2009: pre-construction (baseline) (Bollhöfer et al, 2009; Doering et al 2011);
- 2010: one year after closure (Doering et al 2011); and
- 2012: three years after closure (Bollhöfer et al 2013).

The external gamma dose rate and radon exhalation flux density used in the assessment were the 99th percentile of the above background values calculated from the difference of the 2012 and baseline measurements. These values were 0.03 µGy h^{-1} for external gamma dose rate and 900 mBq m^{-2} s^{-1} for radon exhalation flux density.

Comparison of the 2010 and 2012 measurements indicated that there was no significant difference in external gamma dose rates. However, there was an approximately 3 fold increase in radon exhalation flux densities from 2010 to 2012. This increase may be indicative of deterioration in site radiological characteristics. Potentially, the 0.5 m compacted clay capping that was placed immediately on top of the buried waste has dried and cracked in places, or roots from plants establishing on site have created preferential pathways, allowing more radon from the buried waste to diffuse through and exhale from the soil cover.

2.4 Assessment method

The dose from external gamma radiation was calculated by multiplying the 99th percentile of the above background dose rate with the time spent onsite. The dose from radon progeny inhalation was calculated using the RESRAD-Offsite computer model, with the 99th percentile of the above background radon exhalation flux density used to determine the radon progeny concentration in air on and downwind of the containment for highly stable atmospheric conditions. Full details of the assessment are given in Bollhöfer et al (2013).

3 Results

Table 2 gives the expected maximum doses to a worker and a member of the public from the containment for the assumed exposure scenarios. The results indicate that in both cases the expected maximum dose from all pathways is less than 10 µSv per year for the current radiological characteristics of the containment. The tourist camping received the higher dose due to radon progeny as it was assumed the worker was in the centre of the containment and thereby only exposed to radon expressed from the upwind section, whereas the camper is downwind of the entire containment footprint.

Table 2. Expected maximum above background annual effective doses (µSv) to a worker and the public from the El Sherana airstrip containment.

	External gamma	Inhalation		Ingestion	Total
		Radon progeny	Dust		
Occupational (Park Ranger)	3	1	0	0	4
Public (tourist camping)	0	6	0	0	6

4 Discussion

A dose constraint is *"a prospective and source-related restriction on the individual dose from a source in planned exposure situations ... which serves as an upper bound on the predicted dose in the optimisation of protection for that source"* (ICRP 2007). In the context of proposing or establishing a dose constraint for a source, the implication is that it should be commensurate with the expected maximum dose to an individual from the source based on an assessment that takes into account the characteristics of the source and the scenarios for exposure. However, other factors may also influence the selection of dose constraint, including:

- the possibility of deterioration in site characteristics and capacity for repair;
- the views of interested parties (stakeholders);
- the capability to measure and demonstrate doses below the dose constraint; and
- national and international guidance and good practice elsewhere.

Based on the assessment results of Bollhöfer et al (2013) alone, and assuming stable site characteristics into the future, a dose constraint of around 10 μSv per year would be appropriate for the containment for both workers and the public for the institutional control period. However, there is some evidence to suggest that radiological site characteristics have deteriorated between 2010 and 2012, allowing more radon to diffuse through and exhale from the soil cover. Further increases in radon exhalation from the site would imply higher maximum expected doses than those given in Table 2. A dose constraint greater than 10 μSv per year may therefore be appropriate to compensate for this and still achieve doses that provide an optimised level of protection for workers and the public.

References

ARPANSA 2011. Inspection report. Report number R11/12857. Available from: http://arpansa.gov.au/pubs/regulatory/inspections/R11-12857.pdf

Bollhöfer A, Dunn L, Pfitzner K, Ryan B, Fawcett M & Jones DR 2009. Remediation of the remnants of past uranium mining activities in the South Alligator River Valley. In eriss research summary 2007–2008. eds Jones DR & Webb A, Supervising Scientist Report 200, Supervising Scientist, Darwin NT, 206-211.

Bollhöfer A, Doering C, Medley P & Da Costa L 2013. Assessment of expected maximum doses from the El Sherana airstrip containment, South Alligator River valley, Australia. Internal Report 618, May 2013, Supervising Scientist, Darwin.

Doering C, Bollhöfer A, Ryan B, Sellwood J, Fox T & Pfitzner J 2011. Baseline and post-construction radiological conditions at El Sherana airstrip containment, South Alligator River valley, Australia. Internal Report 592, June, Supervising Scientist, Darwin.

International Commission on Radiological Protection (ICRP) 2007. The 2007 recommendations of the International Commission on Radiological Protection. ICRP Publication 103, Annals of the ICRP 37(2–4).

National Health and Medical Research Council (NHMRC) 1993. Code of practice for the near-surface disposal of radioactive waste in Australia (1992). Radiation Health Series No. 35.

Puhalovich A, Pillai M, McGovern E & Jacobsen N 2006. Groundwater Level Monitoring & Permeability Testing – Candidate Containment Sites (Gunlom Radiological Materials). Draft Report for Parks Australia North prepared by EWL Sciences Pty Ltd. August 2006.